Fluidics Station 400 (Affymetrix) and scanned by Gene Array Scanner (Affymetrix).

In the middle of the project (2004), Affymetrix released ver. 2.0 GeneChip and we switched from RAE230A to 230.2. Two out of seven experiments were performed using the new chips, and they were excluded from the present analysis in order to maintain consistency. Therefore, each time point consisted of 15 measures (3 rats for 5 experiments) in the case of gene expression analysis.

The digital image files were processed by Affymetrix Microarray Suite version 5.0 and the intensities were normalized for each chip by setting the mean intensity to 500 (per chip normalization). The results of the DNA microarray analysis are available upon request (e-mail to turushid@dwc.doshisha.ac.jp).

Statistical analysis

For conventional toxicological parameters, it is common that many unimportant changes with statistical significance are observed because of the large numbers of measurements. In the present study, more than 40 parameters were measured for 8 time points (3, 6, 9, 24 h for single and 3, 7, 14, 28 days for repeated administration). For comparison between methylcellulose and corn oil, we applied Student's t-test with Bonferroni's adjustment for each parameter, i.e., p value was multiplied by 8 and $p<0.01$ was considered to be statistically significant.

For gene expression data, it is problematic to use a standard t-test, because of too many comparisons, but it is also not good to use a too conservative adjustment, because of the small

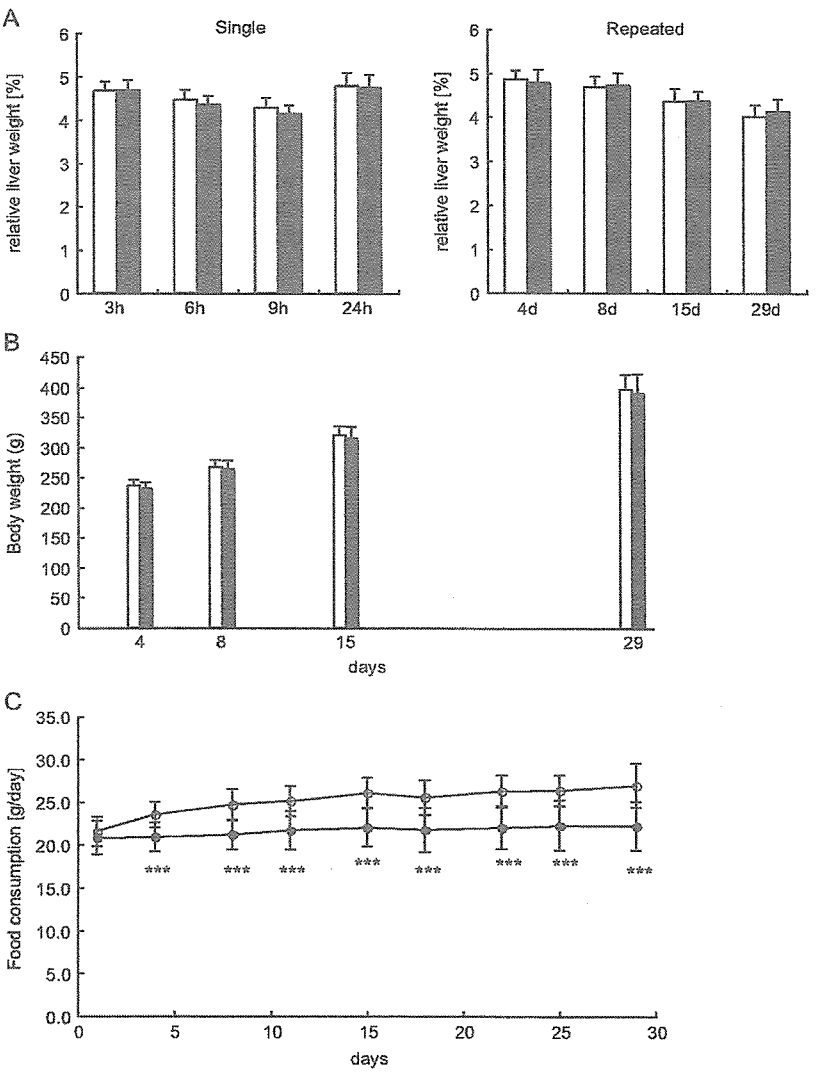

Fig. 1. Effects of different vehicles on relative liver weight, body weight, and food consumption of rats. Liver weight/body weight within 24 h after administration of vehicle and 24 h after the repeated administrations (for 3, 7, 14 and 28 days) of vehicle were measured at autopsy (A). Open and filled columns represent methylcellulose and corn oil, respectively. Body weight 24 h after the repeated administrations (for 3, 7, 14 and 28 days) of vehicle (B) and food consumption measured every 4 days and expressed as g/day (C) are plotted. Again, open and filled symbols represent methylcellulose and corn oil, respectively. Values are expressed as mean± SD of 35 rats each for each time point. Food consumption data were obtained from rats that received either vehicle for 28 days. ***Statistically significant between methylcellulose and corn oil by Student's t-test with Bonferroni's adjustment, at $p<0.001$.

numbers of samples compared with the numbers of genes. In the present study, we considered that the β-error should be small, since our purpose was to pick up the possible vehicle effects on gene expression. Before comparison, the genes that showed less than 20 of the expression value after per chip normalization in all the samples were excluded. Genes extracted were those showing at least 1.5 fold difference between two vehicles, with $p<0.01$ (uncorrected t-test).

Results

It is common that some statistically significant but unimportant differences are observed in toxicological tests where huge numbers of parameters are measured and compared. In the present analysis of the vehicle effect, there appeared to be some differences that could not be ignored. Fig. 1A depicts the relative weight of the liver (liver weight/body weight). As is widely known, this parameter showed a clear circadian rhythm, i.e., it decreases toward the evening (9 h after dosing) and goes back in the next morning (Fig. 1A, left). In the case of rats receiving corn oil, this parameter tended to be lower than that in methylcellulose group at 6 and 9 h after dosing ($p=0.03$ and $p=0.005$, respectively, by standard t-test, but $p=0.24$ and $p=0.04$, respectively, by Bonferroni's adjustment and not significant at $p<0.01$), whereas the values returned to the same level at 24 h after administration. There was no difference in this parameter in the repeated administration, suggesting that the tendency of the decrease in the liver weight by corn oil was not accumulated during repeated dosing (Fig. 1A, right). Fig. 1 shows the body weight change (B)

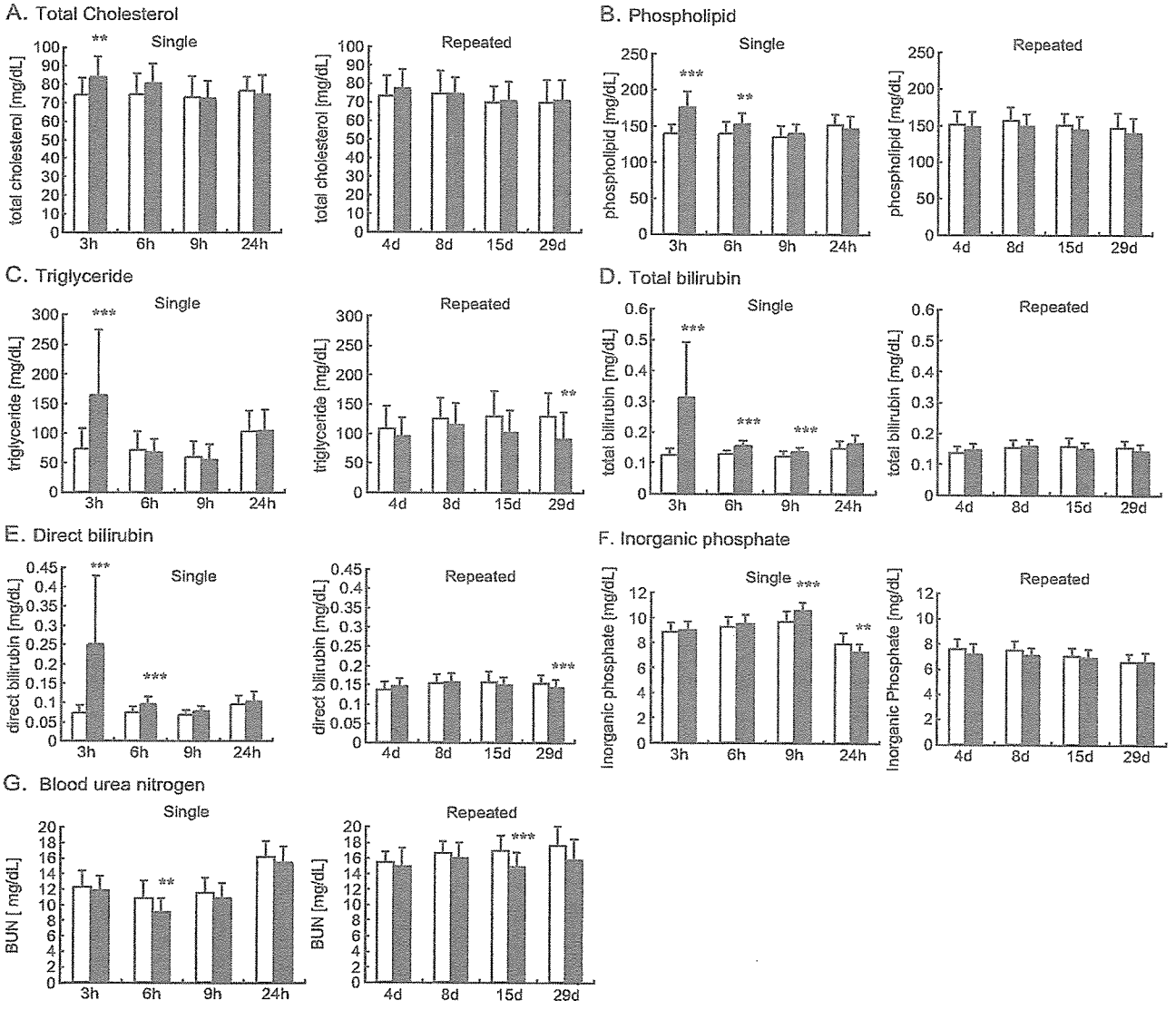

Fig. 2. Blood biochemical parameters in rats receiving methylcellulose or corn oil. Total cholesterol (A), triglyceride (B), phospholipid (C), total bilirubin (D) and direct bilirubin (E), inorganic phosphate (F), and blood urea nitrogen (G) showed a significant difference between methylcellulose (open columns) and corn oil (closed columns) among 36 parameters. Values are expressed as mean ± SD of 35 rats for each time point. Statistically significant between methylcellulose and corn oil by Student's t-test with Bonferroni's adjustment, at $^{**}p<0.01$, $^{***}p<0.001$.

Table 1
List of genes showing at least a 1.5 fold difference with $p<0.01$ (uncorrected t-test) between methylcellulose and corn oil at any point during 24 h after single dose or at 29th day of repeated dose

Probe set ID	Gene title	Gene symbol	3 h	6 h	9 h	24 h	29 d
1367707_at	fatty acid synthase	Fasn	0.995	1.738	1.300	0.722	0.596
1367708_a_at	fatty acid synthase	Fasn	0.982	1.500	1.182	0.826	0.678
1367729_at	ornithine aminotransferase	Oat	1.223	1.140	1.066	0.792	0.653
1367836_at	carnitine palmitoyltransferase 1, liver	Cpt1a	1.325	1.483	1.535	0.888	1.305
1367854_at	ATP citrate lyase	Acly	1.081	1.741	1.295	0.882	0.760
1367946_at	PDZ and LIM domain 1 (elfin)	Pdlim1	0.762	0.661	0.777	0.914	0.977
1367959_a_at	sodium channel, voltage-gated, type I, beta polypeptide	Scn1b	1.042	1.013	1.567	1.613	1.278
1368035_a_at	protein tyrosine phosphatase, receptor type, F	Ptprf	0.935	1.009	0.649	0.920	0.985
1368160_at	insulin-like growth factor binding protein 1	Igfbp1	1.239	0.485	1.238	0.631	1.143
1368272_at	glutamate oxaloacetate transaminase 1	Got1	1.623	0.989	0.965	0.687	0.813
1368275_at	sterol-C4-methyl oxidase-like	Sc4mol	0.902	1.224	1.552	0.929	0.857
1368428_at	X-prolyl aminopeptidase (aminopeptidase P) 2, membrane-bound	Xpnpep2	0.839	0.896	0.668	0.783	0.916
1368435_at	cytochrome P450, family 8, subfamily b, polypeptide 1	Cyp8b1	1.534	1.860	1.570	0.711	0.798
1368458_at	cytochrome P450, family 7, subfamily a, polypeptide 1	Cyp7a1	0.471	1.768	1.310	0.586	0.607
1368569_at	aldo-keto reductase family 1, member B7	Akr1b7	0.197	0.971	0.190	2.782	5.398
1369073_at	nuclear receptor subfamily 1, group H, member	Nr1h4	1.165	1.594	1.190	0.903	1.047
1369195_at	fatty acid binding protein 2, intestinal	Fabp2	0.901	1.135	1.022	1.753	1.753
1369238_at	inhibin beta E	Inhbe	1.441	1.553	1.067	1.034	0.934
1369415_at	basic helix-loop-helix domain containing, class B2	Bhlhb2	1.019	1.814	1.449	0.983	0.862
1369440_at	ATP-binding cassette, sub-family G (WHITE), member 8	Abcg8	0.676	0.538	0.701	0.893	1.440
1369493_at	prolactin receptor	Prlr	0.609	0.958	0.717	1.147	1.975
1369663_at	epoxide hydrolase 2, cytoplasmic	Ephx2	1.073	1.346	1.616	1.196	1.844
1369674_at	purinergic receptor P2X, ligand-gated ion channel, 5	P2rx5	1.930	0.838	0.893	0.811	1.065
1369790_at	tyrosine aminotransferase	Tat	0.771	0.624	1.094	0.735	0.837
1369864_a_at	serine dehydratase	Sds	1.509	0.429	0.872	0.482	0.538
1370024_at	Fatty acid binding protein 7, brain	Fabp7	1.044	0.964	1.057	1.312	1.524
1370336_at	pregnancy-induced growth inhibitor	Okl38	0.615	0.694	0.735	1.091	1.139
1370355_at	stearoyl-Coenzyme A desaturase 1	Scd1	1.206	1.197	1.065	0.904	0.604
1370427_at	platelet derived growth factor, alpha	Pdgfa	1.066	0.912	1.155	0.559	1.097
1371127_at	bone morphogenetic protein 1 (procollagen C-proetinase)	RGD:620739	0.815	1.175	0.950	0.991	1.557
1371234_at	fibrinogen, B beta polypeptide	Fgb	1.165	0.990	0.896	0.894	0.639
1371279_at	histone 2a /// similar to Histone H2A.1	RGD:621437	1.093	0.910	0.798	0.604	0.843
1371595_at	Transcribed locus, weakly similar to XP346694.1 Rattus norvegicus LOC360381 gene	---	0.738	0.639	0.607	0.824	0.938
1371754_at	solute carrier family 25 (mitochondrial carrier, phosphate carrier), member 25	Slc25a25	0.939	0.891	1.187	0.912	0.660
1372188_at	Endothelial cell growth factor 1 (platelet-derived) (predicted)	---	1.043	1.548	1.053	1.187	1.051
1372276_at	Transcribed locus	---	0.941	1.673	1.209	1.340	1.714
1372536_at	Chaperone, ABC1 activity of bc1 complex like (S. pombe) (predicted)	---	0.953	0.973	0.659	0.904	1.082
1374265_at	Similar to arylacetamide deacetylase (esterase) (predicted)	---	0.964	1.221	1.511	0.872	0.853
1374932_at	---	---	0.818	1.705	0.745	1.055	0.897
1375367_at	PDZ and LIM domain 2	Pdlim2	1.283	1.623	1.002	0.870	0.896
1375422_at	---	---	1.094	0.936	1.375	1.039	1.025
1375552_at	---	---	0.889	1.176	0.927	0.932	1.584

Data are expressed as the ratio of gene expression (methylcellulose=1) and columns with significant change are shaded ($N=15$ for each group).

together with food consumption (C). Although both methylcellulose and corn oil groups got weight in the same rate during repeated dosing, food consumption in the corn oil group was significantly lower than that in methylcellulose group by about 15% throughout the period of repeated administration.

Among the hematological and blood biochemical parameters, mean corpuscular hemoglobin concentration (at 15th day), platelets (at 9 h), monocytes (at 3 h), prothrombin time (at 29th day), activated partial thromboplastin time (at 24 h), fibrinogen (at 3 h), chloride (at 3 h) showed statistically significant differences between corn oil and methylcellurose. However, these changes were not considered to be important, since their changes were small and no changes in related parameters were associated. On the other hand, total cholesterol, phospholipids, triglyceride, and bilirubin (both total and direct) were found to be significantly different between vehicle controls (Fig. 2A–E). All of them showed significantly higher values in the corn oil group at 3 h after dosing, and the differences abated or disappeared at 6 h or later. In the repeated administration, the corn oil group showed rather lower values of triglyceride, total and direct bilirubin. Inorganic phosphate showed a significantly higher value in corn oil at 9 h and went down to a lower value than methylcellulose (Fig. 2F). Blood urea nitrogen (Fig. 2G) showed a lower value in corn oil at 6 h and 15th day.

Scatter plots of gene expression between vehicle controls at each time point revealed that most of the genes distributed within a 2-fold range of their 45° line, meaning that few

Table 1 (*continued*)

Probe set ID	Gene title	Gene symbol	3 h	6 h	9 h	24 h	29 d
1375619_at	---	---	1.171	0.667	0.789	0.971	0.756
1375796_at	interferon gamma induced GTPase (predicted)	Igtp_predicted	1.005	0.883	1.021	1.787	0.847
1376313_at	two pore segment channel 2 (predicted)	RGD:1311779	1.040	0.800	0.871	0.991	1.956
1376657_at	immunoglobulin superfamily, member 4A (predicted)	Igsf4a_predicted	1.060	1.749	1.510	0.868	1.022
1376704_a_at	necdin-like 2 (predicted)	Ndnl2_predicted	1.048	0.886	1.061	0.995	0.660
1376892_at	---	---	1.109	0.949	0.854	0.654	0.953
1376958_at	Similar to serine (or cysteine) proteinase inhibitor, clade B, member 9	---	0.456	0.824	1.105	1.206	1.039
1377361_at	---	---	1.004	0.667	0.794	0.890	1.020
1379252_at	Immunoglobulin superfamily, member 4A (predicted)	---	1.083	1.505	1.476	0.861	0.970
1383075_at	cyclin D1	Ccnd1	0.636	0.693	0.945	1.029	1.211
1384178_at	Leucine rich repeat containing 4B (predicted)	---	0.906	0.656	0.890	0.802	0.884
1384288_at	Transcribed locus	---	1.119	0.596	1.136	0.835	1.054
1386041_a_at	Kruppel-like factor	Klf2	1.986	0.850	1.345	1.004	1.053
1386789_at	---	---	1.305	0.611	1.196	1.134	1.003
1387017_at	squalene epoxidase	Sqle	0.927	1.279	1.832	1.058	0.980
1387022_at	aldehyde dehydrogenase family 1, member A1	Aldh1a1	0.769	1.099	0.913	1.039	1.804
1387123_at	cytochrome P450, family 17, subfamily a, polypeptide 1	Cyp17a1	1.003	0.982	1.106	1.309	1.613
1387183_at	carnitine O-octanoyltransferase	Crot	1.058	1.116	1.142	0.914	1.569
1387283_at	myxovirus (influenza virus) resistance 2	Mx2	0.721	0.777	0.503	1.565	1.280
1387307_at	histidine ammonia lyase	Hal	0.903	0.826	0.665	0.819	1.072
1387312_a_at	glucokinase	Gck	1.180	1.610	0.865	0.941	1.077
1387391_at	cyclin-dependent kinase inhibitor 1A	Cdkn1a	1.576	1.373	0.734	0.684	0.892
1387396_at	hepcidin antimicrobial peptide	Hamp	0.731	0.642	1.232	1.145	1.051
1387643_at	fibroblast growth factor 21	Fgf21	1.385	1.919	1.138	1.191	1.157
1387665_at	betaine-homocysteine methyltransferase	Bhmt	1.234	1.064	1.083	0.655	0.850
1387670_at	glycerol-3-phosphate dehydrogenase 2	Gpd2	1.169	1.650	1.430	0.872	0.864
1387730_at	paired box gene 8	Pax8	1.527	1.114	0.991	0.822	0.827
1387809_at	mitogen-activated protein kinase kinase 6	Map2k6	1.017	1.443	1.139	0.622	0.742
1387848_at	3-hydroxy-3-methylglutaryl-Coenzyme A reductase	Hmgcr	0.810	1.306	1.963	1.057	0.876
1388210_at	mitochondrial acyl-CoA thioesterase 1	Mte1	1.085	1.245	1.928	1.099	1.120
1388395_at	G0/G1 switch gene 2 (predicted)	G0s2_predicted	2.129	1.930	1.041	1.204	1.036
1388426_at	sterol regulatory element binding factor 1	Srebf1	0.648	0.787	0.694	0.855	0.885
1388531_at	progesterone receptor membrane component 2 (predicted)	Pgrmc2 predicted	1.032	1.518	1.149	0.938	1.036
1388679_at	TBC1 domain family, member 14 (predicted)	Tbc1d14 predicted	0.815	1.582	1.111	0.883	1.038
1388792_at	growth arrest and DNA-damage-inducible 45 gamma (predicted)	Gadd45 gpredicted	0.340	1.095	0.994	0.669	0.595
1388872_at	Isopentenyl-diphosphate delta isomerase	Idi1	1.029	1.077	1.772	1.249	0.870
1388924_at	angiopoietin-like protein 4	Angptl4	2.172	1.589	1.105	0.673	0.990
1389161_at	Transcribed locus	---	1.547	1.566	1.153	0.819	1.014
1389253_at	vanin 1 (predicted)	Vnn1 predicted	1.127	1.614	1.846	1.232	1.650
1389430_at	Transcribed locus	---	0.917	1.198	1.517	0.863	1.008
1390383_at	adipose differentiation-related protein	ADRP	1.296	1.784	0.870	0.952	0.913
1390607_at	nNOS-intereacting DHHC-containing Dem protein-L	RGD:1303254	0.936	1.463	1.509	0.691	0.878
1390662_at	Ab2-427	---	0.594	0.996	0.819	1.114	0.980
1392607_at	Transcribed locus	---	0.756	0.855	0.725	0.441	1.298

genes were affected by the vehicle (data not shown). Table 1 shows the list of genes that showed at least a 1.5-fold difference between vehicles with $p<0.01$ either in single dose experiment or in the 29th day of repeated dosing. Many of the genes listed are related to lipid metabolism. They were usually up-regulated by corn oil between 3 and 9 h after dosing and returned to the same level or lower at 24 h and at the 29th day. However, there were some exceptional cases, such as aldo-keto reductase 1B7 (down-regulated at 3 and 9 h but up-regulated at 24 h and 29th day), or aldehyde dehydrogenase 1A1 (only up-regulated after repeated administration). Among the genes in Table 1, there are interesting ones, i.e., CYP7A1, CYP8B1, 3-hydroxy-3-methylglutaryl-Coenzyme A reductase, fatty acid synthase, squalene epoxidase, angiopoietin-like protein 4, which are selected and shown as graphs in Fig. 3A–F. The former 5 genes all showed a circadian rhythm in that their expression in the afternoon to the evening was higher than that in the morning to noon. The administration of corn oil appeared to increase this peak. On the other hand, angiopoietin-like protein 4 showed constant expression during the day in methylcellulose, whereas corn oil markedly increased the expression of this gene at 3 and 6 h of administration.

As is obvious from Figs. 1A and 3, there exists a circadian rhythm in rat liver. In order to examine whether the observed changes were due to a disturbance in the basic rhythm, expression of various clock genes were checked and we found that the rhythm (other than that related to lipid metabolism) was relatively unaffected. As typically representative of clock genes, the expression patterns of period 2, D site albumin

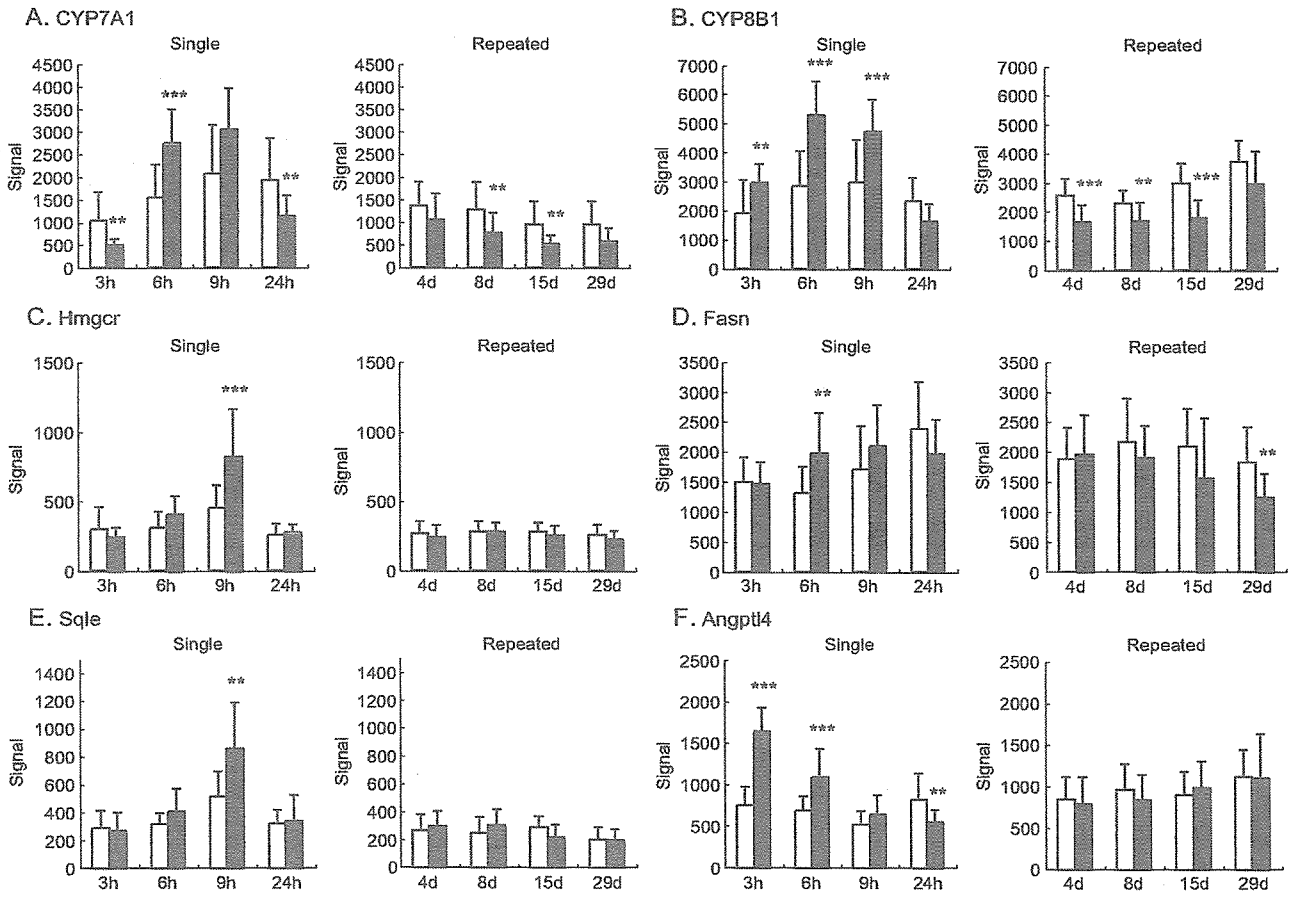

Fig. 3. Expression changes of CYP7A1 (A, Affymetrix ID 1368458_at), CYP8B1(B, Affymetrix ID 368435_at), 3-hydroxy-3-methylglutaryl-Coenzyme A reductase (C, Affymetrix ID 1387848_at), fatty acid synthase (D, Affymetrix ID 1367708_a_at), squalene opixidase (E, Affymetrix ID 1387017_at) and angiopoietin-like protein 4 (F, Affymetrix ID 1388924_at) are shown. Open and filled symbols represent methylcellulose and corn oil, respectively. Values are expressed as mean ± SD of 15 rats of each for each time point. Statistically significant between methylcellulose and corn oil by uncorrected Student's *t*-test at $^{**}p<0.01$, $^{***}p<0.001$.

promoter binding protein, and arylhydrocarbon receptor nuclear translocator-like are shown in Fig. 4A–C.

Discussion

The ultimate goal of our project is to create a gene expression database for prediction of hepatotoxicity in the early stage of drug development. For this purpose, it was desirable that the vehicle for suspending drugs was unified to be methylcellulose. However, there are many test compounds with poor dispersibility, and strong detergents or organic solvents are undesirable because of their potent bioactivity, so we inevitably chose corn oil as a vehicle for the highly hydrophobic compounds.

Corn oil contains 9.2 kcal/g and supplies 10.1 kcal/day for 7-week-old rats (5 ml/kg corresponds to 1.1 g for 250 g body weight). Rats around this age consume about 25 g diet per day in the present study (Fig. 1C), which corresponds to about 90 kcal/day (CRF-1 carries 3.6 kcal/g), meaning that the administered corn oil is equal to about 11% of the total calories. Moreover, this is administered once in the morning when the feeding behavior of the rat is normally inactive. Then we were concerned that the difference between corn oil and methylcellulose cannot be ignored. In fact, the food intake of the rats in the corn oil group was significantly decreased by about 15% compared with methylcellulose group without any changes in body weight. This suggests that the rats self-controlled their total calorie intake to a constant level and so corresponding gene expression changes should have occurred.

In the acute phase, total cholesterol, triglyceride, phospholipids, and bilirubin were elevated 3 h after the administration of corn oil, which were considered to be due to rapid absorption of oil. We are not sure why plasma bilirubin was increased; it might reflect an increase in the absorption of bile components when large amounts of lipid were absorbed in the form of micelle. These parameters all returned to the same level as in the methylcellulose group 6–9 h after administration. In the repeated dose experiments, which correspond to 24 h after dosing, triglyceride and bilirubin were decreased in the corn oil group, suggesting that some adapting system lowering plasma lipid was induced during a continuous elevation of lipid component in the diet.

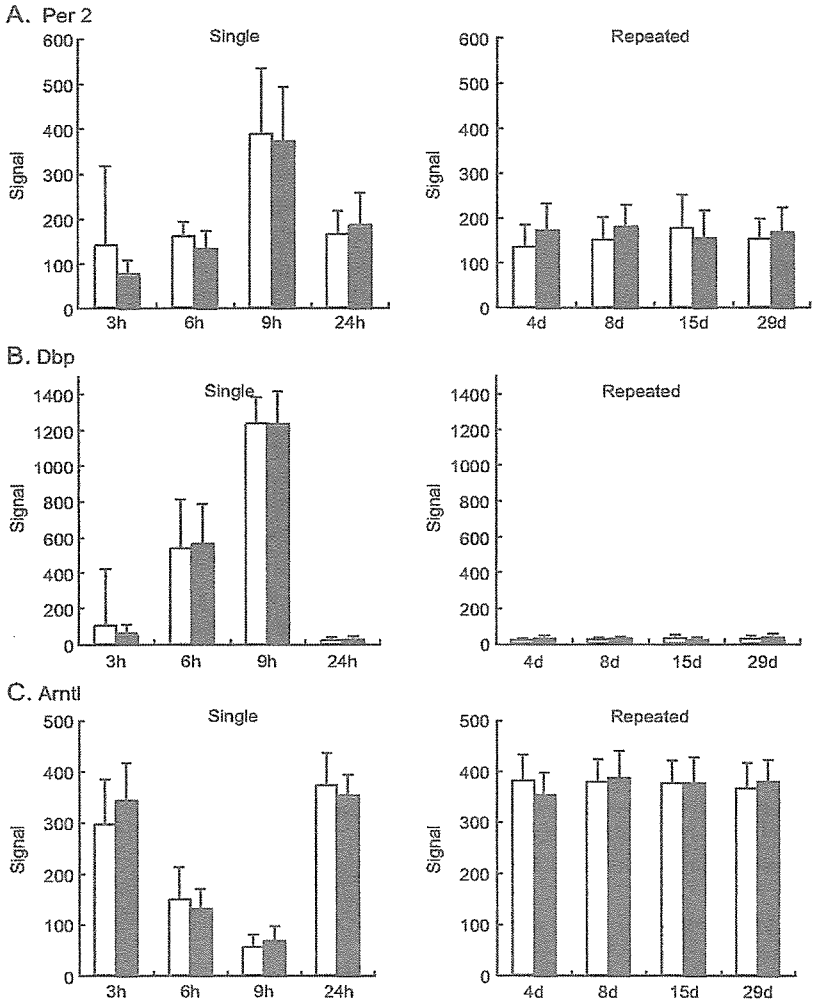

Fig. 4. Expression patterns of representative clock genes, period 2 (A, Affymetrix ID 1368303_at), D site albumin promoter binding protein (B, Affymetrix ID 1387874_at), and arylhydrocarbon receptor nuclear translocator-like (C, Affymetrix ID 1370510_a_at) are shown. Open and filled symbols represent methylcellulose and corn oil, respectively. Values are expressed as mean±SD of 15 rats for each time point. No statistically significant difference was observed between methylcellulose and corn oil at any time point.

The change in gene expression in the liver was more complex. Although the numbers of differentially expressed genes were small in respect of the total 16,000 probe sets, there were still considerable numbers of genes showing different patterns between vehicles, most of which were related to lipid metabolism. In the corn oil-treated group, the expression of CYP7A1 (cholesterol 7α hydroxylase), the rate-limiting enzyme of bile acid synthesis or elimination of cholesterol (Mast et al., 2005), showed a clear circadian rhythm as reported (Kai et al., 1995; Ishida et al., 2000), and it was lower at 3 h but higher at 6 and 9 h than that in the methylcellulose group. The expression was then lowered again at 24 h after dosing, and this pattern appeared to continue during repeated administration, i.e., the expression value in the corn oil group stayed about 60% of those in the methylcellulose group until the 29th day. On the other hand, CYP 8B1 (cholesterol 12α hydroxylase), which catalyzes the synthesis of cholic acid and controls the ratio of cholic acid over chenodeoxycholic acid in the bile, showed a less marked but obvious circadian pattern as reported (Ishida et al., 2000). It showed a continuously higher expression from 3 to 9 h than methylcellulose, returned to the same level at 24 h, and no difference was observed in the repeated dosing. These changes were considered to be the reflection of the transiently high consumption of bile due to the bolus injection of corn oil.

The rate-limiting enzyme of cholesterol biosynthesis, 3-hydroxy-3-methylglutaryl-Coenzyme A reductase, also showed a circadian rhythm and the administration of corn oil markedly increased its expression at 9 h. At this point, squalene epoxidase and sterol-C4-methyloxidase were also increased. The former is a microsomal enzyme that catalyzes the oxidation of squalene to 2,3-oxidosqualene, the last reaction of non-sterol metabolites in the cholesterol biosynthesis pathway (Hidaka et al., 1990). The latter is known as one of the components essential for sterol biosynthesis in yeast (Darnet and Rahier, 2003), and it used to be termed neurorep1 and was discussed in relation to the repair

process of damaged neurons (Uwabe et al., 1997). Looking at the high expression level in liver and induction by corn oil alone, we considered that the induction of sterol-C4-methyloxidase was a general phenomenon related to lipid metabolism rather than neurophysiology.

One noticeable gene is angiopoietin-like protein 4, which was recently shown to be involved not only in lipid metabolism via inhibition of lipoprotein lipase activity (Yoshida et al., 2002) but also in various diseases (Xu et al., 2005). It was reported that its expression in adipose tissue and liver was affected by the nutrient status, e.g., induced by fasting (Ge et al., 2005). In the present study, this gene was markedly up-regulated at 3–6 h after corn oil treatment and returned to the same level as methylcellulose at 9 h or later. It is of interest to elucidate why oil intake resembles fasting in case of angiopoietin-like protein 4 expression.

Fatty acid synthase was up-regulated by corn oil at 6 h after dosing and then returned to the same level as methylcellulose, whereas it was down-regulated (about 60% of methylcellulose) after repeated administration. In contrast, fatty acid binding protein family members, involved in lipid uptake, were up-regulated 24 h after single and repeated administrations of corn oil. These reactions in the repeated phase are considered to be adaptive responses suitable for lipid intake. In addition to these two enzymes, there were genes showing significantly different expression in the corn oil group at 29th day, i.e., serine dehydratase, ornithine aminotransferase, stearoyl CoA desaturase, aldehyde dehydrogenase 1A1, and epoxide hydroxylase 2. Of these, the latter two were up-regulated whereas the others were down-regulated.

The increase of aldehyde dehydrogenase and epoxide hydroxylase is considered to be favorable for the condition of high lipid diet, since both enzymes are reported to be involved in the detoxication of the metabolites associated with lipid metabolism (Choudhary et al., 2005; Newman et al., 2005). As for the down-regulated genes, the decrease of fatty acid synthase and stearoyl CoA desaturase, both are in the pathway of fatty acid synthesis, which might reflect a decrease in the need of fatty acid. Serine dehydratase and ornithine aminotransferase are known to be induced by high protein diet, glucagon, or glucocorticoid (Hunter and Harper, 1977; Bourdel et al., 1983). Based on the present data, it is difficult to conclude whether the change was due to the relative reduction of protein in the diet, or to the secondary change in endocrinological status. Moreover, it should be noted that the circadian pattern could not be obtained in the present experiments of repeated administration. Although most of the observed changes could be interpreted as an adaptation for the rapid absorption of oil from the gut in the acute phase and for the continuously elevated composition of lipid in the food in the chronic phase, it is difficult to map all the changes to various metabolic pathways, and to give reasonable explanations. Further confirmation is obviously needed, but the present study has supplied many valuable suggestions.

Many of the genes affected by corn oil treatment exhibit their own circadian rhythm generally with low expression at 3 h (around noon), increasing from 6 h (late afternoon) to 9 h (evening), and returning to low expression at 24 h (morning) of dosing. There is a long blank period between 9 and 24 h after dosing, as it was practically impossible to perform measurements after midnight in the present project. It was therefore possible that the actual peak of some genes occurred between 9 and 24 h after dosing, or midnight. We were concerned that the compulsory administration of oil in the morning disturbs not only feeding behavior but also the circadian rhythm itself. However, it was confirmed that the expression patterns of representative clock genes were unaffected, suggesting that changes in gene expression were not due to the disturbance of the original circadian rhythm. Moreover, the expression levels of clock genes in repeated dosing (corresponding to the 24 h value) were also unchanged, suggesting that disturbance of the circadian rhythm during repeated administration of oil was unlikely.

The present analysis of the data in our database would provide useful information for future experiments to elucidate the detailed mechanism of lipid metabolism. It also provides valuable information for the analysis of the activity of compounds when a comparison of chemicals dosed with different vehicles is made. Since the data accumulated in our database appeared to be of high quality and reproducibility, at least in terms of the effect of vehicles, we expect that drug actions, especially related to toxicity, may be sensitively detected using our database.

Acknowledgements

This study was supported in part by a grant from the Ministry of Health, Labour and Welfare (H14-Toxico-001).

References

Bourdel, G., Hitier, Y., Lardeux, B., Girard-Globa, A., 1983. Activity of several enzymes of amino acid catabolism in the liver of rats fed protein as a meal. Reproduction Nutrition Development 23, 875–881.

Choudhary, S., Xiao, T., Srivastava, S., Zhang, W., Chan, L.L., Vergara, L.A., Van Kuijk, F.J., Ansari, N.H., 2005. Toxicity and detoxification of lipid-derived aldehydes in cultured retinal pigmented epithelial cells. Toxicology and Applied Pharmacology 204, 122–134.

Darnet, S., Rahier, A., 2003. Enzymological properties of sterol-C4-methyl-oxidase of yeast sterol biosynthesis. Biochimica et Biophysica Acta 1633, 106–117.

Ge, H., Cha, J.Y., Gopal, H., Harp, C., Yu, X., Repa, J.J., Li, C., 2005. Differential regulation and properties of angiopoietin-like proteins 3 and 4. Journal of Lipid Research 46, 1484–1490.

Hidaka, Y., Satoh, T., Kamei, T., 1990. Regulation of squalene epoxidase in HepG2 cells. Journal of Lipid Research 31, 2087–2094.

Hunter, J.E., Harper, A.E., 1977. Induction of pyridoxal phosphate-dependent enzymes in vitamin B-6 deficient rats. Nutrition 107, 235–244.

Ishida, H., Yamashita, C., Kuruta, Y., Yoshida, Y., Noshiro, M., 2000. Insulin is a dominant suppressor of sterol 12 alpha-hydroxylase P450 (CYP8B) expression in rat liver: possible role of insulin in circadian rhythm of CYP8B. Journal of Biochemistry (Tokyo) 127, 57–64.

Kai, M.-H., Eto, T., Kondo, K., Setoguchi, Y., Higashi, S., Maeda, Y., Setoguchi, T., 1995. Synchronous circadian rhythms of mRNA levels and activities of cholesterol 7 alpha-hydroxylase in the rabbit and rat. Journal of Lipid Research 36, 367–374.

Mast, N., Graham, S.E., Andersson, U., Bjorkhem, I., Hill, C., Peterson, J., Pikuleva, I.A., 2005. Cholesterol binding to cytochrome P450 7A1, a key enzyme in bile acid biosynthesis. Biochemistry 44, 3259–3271.

Newman, J.W., Morisseau, C., Hammock, B.D., 2005. Epoxide hydrolases: their roles and interactions with lipid metabolism. Progress in Lipid Research 44, 1–51.

Urushidani, T., Nagao, T., 2005. Toxicogenomics: the Japanese initiative. In: Borlak, J. (Ed.), Handbook of Toxicogenomics—Strategies and Applications. Wiley-VCH, pp. 623–631.

Uwabe, K., Gahara, Y., Yamada, H., Miyake, T., Kitamura, T., 1997. Identification and characterization of a novel gene (neurorep 1) expressed in nerve cells and up-regulated after axotomy. Neuroscience 80, 501–509.

Waring, J.F., Ulrich, R.G., Flint, N., Morfitt, D., Kalkuhl, A., Staedtler, F., Lawton, M., Beekman, J.M., Suter, L., 2004. Interlaboratory evaluation of rat hepatic gene expression changes induced by methapyrilene. Environmental Health Perspectives 112, 439–448.

Xu, A., Lam, M.C., Chan, K.W., Wang, Y., Zhang, J., Hoo, R.L., Xu, J.Y., Chen, B., Chow, W.S., Tso, A.W., Lam, K.S., 2005. Angiopoietin-like protein 4 decreases blood glucose and improves glucose tolerance but induces hyperlipidemia and hepatic steatosis in mice. Proceedings of the National Academy of Sciences of the United States of America 102, 6086–6091.

Yoshida, K., Shimizugawa, T., Ono, M., Furukawa, H., 2002. Angiopoietin-like protein 4 is a potent hyperlipidemia-inducing factor in mice and inhibitor of lipoprotein lipase. Journal of Lipid Research 43, 1770–1772.

Available online at www.sciencedirect.com
SCIENCE DIRECT®
ELSEVIER
Experimental and Molecular Pathology xx (2006) xxx–xxx
Experimental and Molecular Pathology
www.elsevier.com/locate/yexmp

Gene expression profiles of drug-metabolizing enzymes (DMEs) in rat liver during pregnancy and lactation

Xi Jun He *, Hirofumi Yamauchi, Kazuhiko Suzuki, Masaki Ueno, Hiroyuki Nakayama, Kunio Doi

Department of Veterinary Pathology, Graduate School of Agricultural and Life Sciences, The University of Tokyo, 1-1-1 Yayoi, Bunkyo-ku, Tokyo 113-8657, Japan

Received 10 April 2006, and in revised form 27 April 2006

Abstract

A cDNA microarray analysis was conducted to examine hepatic gene expression profiles in pregnant and lactating F344 rats compared to a virgin control group using an Affymetrix GeneChip system. Of the approximately 16000 gene transcripts interrogated, more than 1000 were significantly modified in their expression when detected either in late pregnancy (19 days of gestation, GD 19, 513 genes upregulated and 579 downregulated) or on the day of delivery (postpartum 0 day, PPD 0, 497 upregulated and 733 downregulated). Particular interest was paid to the gene expression of drug-metabolizing enzymes (DMEs) and nuclear receptors (NRs). Though the expression of a few genes, those for CYP7A1, CYP51 and Sultx3, increased, the expression of a number of genes encoding DMEs (Phase I and Phase II) and NRs decreased during pregnancy and lactation. Changes in the expression of 9 genes encoding DMEs and NRs were confirmed by quantitative real-time PCR. For all 9 genes tested, overall, the results of the microarray and real-time PCR analyses were in agreement. This is the first application of a microarray analysis to the expression profiling of genes encoding DMEs and NRs in the liver of pregnant and lactating rats. When combined with other studies, the present study may provide a basis for investigating the mechanism of toxicity of environmental or other nonphysiologic chemicals to the fetus and mother and drug safety during pregnancy and lactation.

Introduction

Physiological and anatomical alterations develop in many organ systems during the course of pregnancy and delivery, and all metabolic functions are increased during pregnancy to provide for the demands of the fetus, placenta, and uterus as well as for the gravida's increased basal metabolic rate and oxygen consumption (Christopher and Gertic, 1998). The dynamic physiological changes that occur in the maternal–placental–fetal unit during pregnancy influence the pharmacokinetic processes of drug absorption, distribution, and elimination (Loebstein and Koren, 1997). This may be due to changes in the activity of hepatic drug-metabolizing enzymes (DMEs). Previous studies have demonstrated that normal pregnancy is associated with a decrease in total cytochrome P450 (CYP450) content and/or reduced activity of microsomal drug-metabolizing enzyme in the liver (Dean and Stock, 1975; Dean et al., 1989; Feuer and Liscio, 1969; Guarino et al., 1969; Neale and Parke, 1973). A recent study by He et al. also suggests that pregnancy is associated with decreases in the level of some CYP450 isozymes (CYPs) (He et al., 2005b).

Lactation is a physiological state associated with significant metabolic adaptations and changes in the energy balance (Xiao et al., 2004). In lactating animals, the production of milk results in increased competition for available nutrients with other processes such as the formation of body reserves. One study showed greater variability in pharmacokinetic parameters in the postpartum period than in nonpregnant women or normal volunteers (Frederiksen, 2001). A few studies have been performed on the effects of lactation on tissue metabolism and activities of certain enzymes. Smith has demonstrated that the activities of some enzymes in the rat liver are influenced by pregnancy and lactation (Smith, 1975). Based on their observations, Abel et al. have suggested that drug disposition is altered during lactation (Abel et al., 1979). Data from He et al. show that in the rat, lactation is accompanied by decreases in the protein levels of some CYPs.

* Corresponding author. Fax: +81 3 5841 8185.
E-mail address: aaa37172@mail.goo.ne.jp (X.J. He).

0014-4800/$ - see front matter © 2006 Elsevier Inc. All rights reserved.
doi:10.1016/j.yexmp.2006.05.002

There have been a number of studies in rats on the molecular alterations during rat pregnancy and lactation (Escalada et al., 1996; Jahn et al., 1991; Sakaguchi et al., 1998; Travers et al., 1993). However, little is known about the full extent and importance of alterations in gene expression in the liver during pregnancy and lactation, especially the expression of genes encoding DMEs. To better understand the molecular events associated with pregnancy, the expression of genes encoding DMEs (Phase II drug-metabolizing enzymes and CYP450) has been profiled in pregnant rats treated with pregnenolone-16alpha-carbonitrile and/or phenobarbital (Ejiri et al., 2005a,b). However, as the gene expression was a response to a nonphysiologic substance, the data may be of limited use when referring to physiological conditions.

We used a cDNA microarray to acquire a comprehensive profile of pregnancy- and lactation-induced transcriptional adaptations in rat liver. Particular interest was paid to the expression profiles of the genes encoding DMEs and nuclear receptors (NRs). The changes in the expression of nine of the genes were confirmed using the quantitative real-time PCR method. Increased oxidative stress during pregnancy and lactation has been discussed as a cause of the reduction in protein levels of some CYP isozymes in our previous studies (He et al., 2005a,b). The expression data for genes associated with oxidative stress were also examined.

Materials and methods

Pregnant and age-matched virgin Fischer 344 rats (F344, 11 weeks of age), purchased from Saitama Experimental Animal Co. (Saitama, Japan), were used in this study. The day a vaginal plug was recognized was designated as day 0 of gestation. The rats were housed individually in plastic cages in an animal room maintained at 23°C ± 2°C and 55% ± 5% humidity with a 14-h/10-h light/dark cycle, and fed pellets (MF, Oriental Yeast Co., Ltd., Tokyo, Japan) and water ad libitum. Maternal liver tissue was collected on days 13 and 19 of gestation (GD), the day of delivery (PPD 0), and day 14 postpartum (PPD 14). The age-matched virgin rats were used as controls. All procedures were carried out in accordance with a protocol approved by the Animal Care and Use Committee of the Graduate School of Agricultural and Life Science, The University of Tokyo.

Isolation of total RNA

The liver slices were immediately submerged in RNA*later* RNA Stabilization Reagent (QIAGEN, CA, USA). After being incubated at 4°C overnight, samples were stored at −80°C until total RNA was prepared. Total RNA was extracted and purified using a RNeasy Mini Kit (QIAGEN) according to the manufacturer's instructions. The integrity of the purified total RNA was determined by denaturing agarose gel electrophoresis.

cDNA microarray analysis

cDNA was synthesized with 10 μg of total RNA, using a SuperScript Double Stranded cDNA Synthesis Kit (Invitrogen, CA) with an oligo (dT) primer containing a T7 RNA polymerase promoter (Affymetrix, CA). Following synthesis of the second strand, the reaction mixture was extracted with phenol–chloroform–isoamyl alcohol, and the double-stranded cDNA was precipitated with ethanol. The DNA was resuspended in RNase-free water and used to synthesize biotinylated cRNA with a 3′-Amplification Reagents for IVT Labeling Kit (Affymetrix). Following a 16-h incubation at 37°C, the resultant biotin-labeled cRNA was purified with RNeasy columns (Qiagen) and eluted in 20 μl of RNase-free water. A total of 20 μg of biotinylated cRNA was fragmented and stored at −20°C prior to use for hybridization. The hybridization solution was prepared using a GeneChip Eukaryotic Hybridization Control Kit (Affymetrix) and was hybridized to the Affymetrix Rat Expression Array 230 A at 45°C for 16 h in a GeneChip Hybridization Oven 640 (Affymetrix). The chips were washed and stained using a Fluidics Station (Affymetrix) and scanned with the GeneArray Scanner.

Microarray data analysis and presentation

Images from the scanned chips were processed and analyzed using Affymetrix Microarray Analysis Suite (MAS) 5.0 and Microsoft Excel. For analysis of the different liver tissue target RNA samples (GD 13, GD 19, PPD 0 and PPD 14), values for gene expression in the samples of nonpregnant virgin controls were set as the baseline. After global normalization was performed for each experimental datum, the fold change was derived as the ratio of average differences from one experimental array compared to a control array. Statistical analysis was performed with Student's *t* test or Welch's *t* test. Genes with low reliability (detection *P* value > 0.05) were excluded from the analysis.

Quantitative real-time RT-PCR

Total RNA was prepared as described above. Primer pairs were designed for each gene using Primer Express v2.0. software (Perkin-Elmer Applied Biosystems), except the primers for GAPDH. All primers were purchased from Sigma-Aldrich (Sigma, Japan). The primer sequences and annealing temperature are listed in Table 1. Quantitative real-time PCR was performed with the SYBR Green Master Mix following the manufacturer's instructions (Toyobo, Osaka, Japan). Samples were processed in triplicate on an ABI PRISM 7900HT Sequence Detection System. The thermal-cycling condition were as follows: 40 cycles of a three-step PCR (95°C for 15 s, 60 or 64°C for 15 s, and 72°C for 45 s) after an initial denaturation (95°C for 2 min). To quantify the expression of a gene, we generated a standard curve using known copy numbers (10, 50, 100, 500, 1000 and 5000) of the genes and the GAPDH transcript. And the gene expression level in each cDNA sample was normalized to the internal GAPDH levels.

Table 1
Primer sequences used in the real-time PCR analysis

Genes	Sense primer sequence (5′–3′)	Antisense primer sequence (5′–3′)	Annealing temperature (°C)
CYP2j3	CTTCTCCAGTGGCCAGACATG	GTCATCAGGGCAAACCTCCTT	60
CYP4f4	ATGATCCCTTCCGCTTCGAC	CCAGAGGTGACCTGTCCTTGATA	60
CYP27	AAGTCTGTGTCCCGCATCGTC	GCGTAGGCTCACCTTCTTGCT	64
Nr1i3	CCAGACCTCTTGGGATGCATT	CGGGTACCAGCACTTTACCCT	60
Nr0b2	GGATTTCCTCGGTTTGCATACA	AAGGGCCTGCTGGACAGTTAG	60
Gstm3	CCTCTTCTTGCTGTTTCCCGA	GGACACAGCACACCTTGCTCA	60
Gstt1	TCGCGCTATTTATATCTTCGCC	TGCATCTGGAACGGGATATTG	64
Ephx1	GGGCATCATGGTCCATAAACA	CCAGTGGGCACAAAGACCTTC	64
Cyp2a1	TGTCACTGCTGCAGATGATGG	TGGGTGAAGCTGCAAATCTGTT	64

Results and discussion

Gene expression profiles of rat liver during pregnancy and lactation

The cDNA microarrays used in this study contain 15,924 transcripts. We profiled the gene expression in rat liver collected at four different stages from early pregnancy (GD 13) to the peak of lactation (PPD 14). The age-matched virgin rats were used as controls. A comparison of the distribution of gene expression patterns revealed greater differences in the control group than the experimental groups. Of approximately 16,000 gene transcripts examined, more than 1000 were significantly modified in their expression either in late pregnancy (GD 19, 513 upregulated and 579 downregulated) or at delivery (PPD 0, 497 upregulated and 733 downregulated). In contrast, fewer modified genes were detected on GD 13 (246 upregulated and 129 downregulated) and PPD 14 (97 upregulated and 275 downregulated) (Fig. 1). The majority of genes modified in their expression at the four different stages were found to be involved in biological processes or molecular functions or to encode cellular components using GenMAPP software (http://www.GenMAPP.org) (data not shown).

The global approach using the microarray analysis revealed that the extent of the changes in gene expression was correlated with distinct stages of pregnancy and lactation. This probably reflects maternal physiologic changes such as the balance between various hormones. In humans, late pregnancy and the early postpartum period are also known to be associated with abrupt changes in levels of several hormones (Elenkov et al., 2001) supporting the gene profiles presented here. In the current study, over 85% of all the genes modified during either pregnancy or lactation showed a changed in expression of less than 2-fold, indicating that the magnitude of the change is small.

Gene expression data for Phase I DMEs

Phase I DMEs consist primarily of the cytochrome P450 (CYP) superfamily of microsomal enzymes, which are found abundantly in the liver, gastrointestinal tract, lung, and kidney. This superfamily comprises families and subfamilies of enzymes classified by amino acid sequence identity or similarity (for

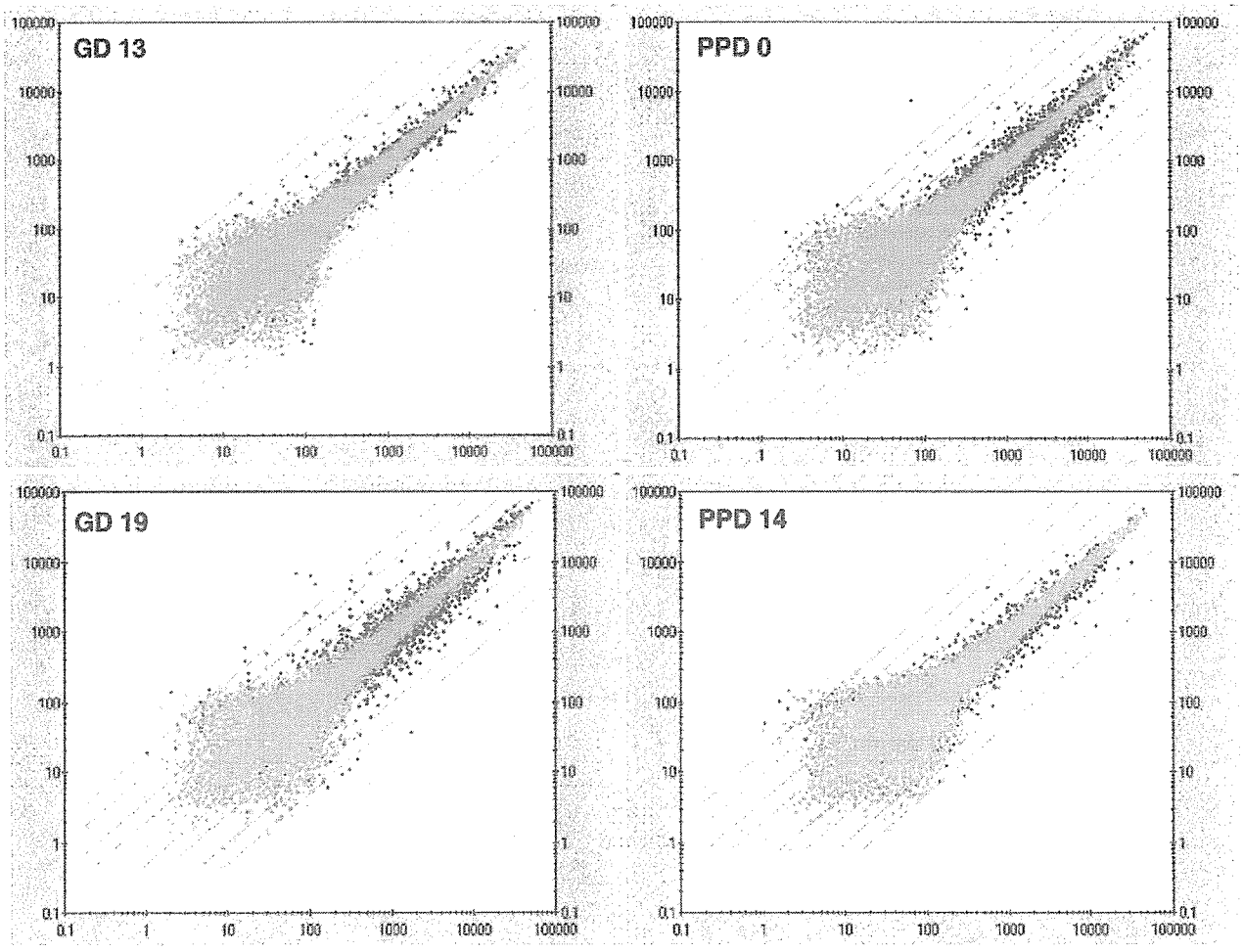

Fig. 1. The average difference distribution of fold changes of gene expression as shown by scatter plots. The control signal values are plotted for the baseline file on the *x*-axis, and the experimental signal values, on the *y*-axis. The upregulated genes are shown in *red* and the downregulated genes in *blue*. The nonregulated genes are shown in *yellow*. Gray lines indicate the magnitude of change with intervals of 2-, 8-, 10- and 20-fold relative to baseline.

Table 2
Modified genes for phase I DMEs (CYPs)

	Accession number	GeneBank definition and comment	Fold change			
			GD 13	GD 19	PPD 0	PPD 14
Downregulated	NM_031543.1	Cytochrome P450, subfamily 2e1 (ethanol-inducible) (Cyp2e1)		−1.42		
	NM_012730.1	Cytochrome P450, subfamily IID2 (Cyp2d2)		−2		
	U04733.1	Cytochrome P450 arachidonic acid epoxygenase (cyp 2C23)		−2		
	NM_031576.1	P450 (cytochrome) oxidoreductase (Por)		−2	2.3	−1.8
	NM_134369.1	Cytochrome P450 monooxygenase CYP2T1 (Cyp2t1)		−2.14	−1.8	
	NM_031241.1	Cytochrome P450, 8b1		−2.83		
	K02422.1	Cytochrome P450, subfamily I (aromatic compound-inducible), member A2 (Q42, form d)	−1.32	−1.41	−1.74	−1.74
	NM_019303.	Cytochrome P450, subfamily IIF, polypeptide 1 (Cyp2f1)		−1.93	−2.38	−1.27
	NM_016999	Cytochrome P450, subfamily IVB, polypeptide 1 (Cyp4b1)		−2		
	NM_012692	Cytochrome P450 IIA1 (hepatic steroid hydroxylase IIA1) gene (Cyp2a1)		−2	−1.93	
	NM_012692.1	Cytochrome P450 IIA1 (hepatic steroid hydroxylase IIA1) gene (Cyp2a1)		−2	−2.14	
	M73231.1	CYP 27	−1.87	−2.3		
	M25143.1	Cytochrome P450CMF1b		−2	−1.74	
	U39206.1	Cytochrome P450 4F4 (CYP4F4)	−1.52	−2		
	AB008424.1	mRNA for CYP2D3		−2.46	−1.87	
	U39943.1	Cytochrome P450 monooxygenase (CYP2J3)	−1.46	−2.46	−1.57	
	AI454613	Cytochrome P450, 2b19	−2.14	−2.64	−1.32	
	U39208.1	Cytochrome P450 4F6 (CYP4F6)			−1.87	
	M33936.1	Cyp4a locus, encoding cytochrome P450 (IVA3) mRNA				−1.62
	J03867.1	NADH-cytochrome b-5 reductase mRNA			−2.07	
	NM_019623.1	Cytochrome P450 4F1 (Cyp4f1)			−1.68	
Upregulated	NM_130408.1	Cytochrome P450, 26, retinoic acid (Cyp26)	1.80			
	M18336.1	Cytochrome P450, 2c37			1.32	
	NM_012942.1	Cytochrome P450 (cholesterol hydroxylase 7 alpha) (Cyp7a1)	1.46		4.14	
	NM_012753.1	Cytochrome P450, subfamily XVII (Cyp17)			4.29	
	BG664123	Cytochrome P450 Lanosterol 14 alpha-demethylase		1.62		1.80
	NM_012941.1	Cytochrome P450 Lanosterol 14 alpha-demethylase (Cyp51)	1.32	1.80		1.68
	BG664123	Cytochrome P450 Lanosterol 14 alpha-demethylase		1.62		1.87
	AI407454	P450 (cytochrome) oxidoreductase			1.8	

review, see Xu et al., 2005). Livers of pregnant and lactating rats were used to examine in more detail the specific genes associated with DMEs to investigate the induction of DMEs in these physiologic states (Table 2).

The major differences in the gene expression of Phase I DMEs occurred either in late pregnancy or at delivery (a total of 29 genes modified, 20 and 17 differentially expressed, respectively), whereas only moderate differences were found in early pregnancy and at peak lactation (only 8 and 7 genes differentially expressed, respectively). Interestingly, most of the downregulated genes belong to the CYP2 family, and no CYP3 family gene was modified at any of the four stages. Within the P450 superfamily, the CYP2 family is the largest and most diverse group (Nelson et al., 1993). This family, whose members are mainly expressed in the liver, contains many of the drug-metabolizing isoforms and also some of the enzymes involved in the metabolism of endogenous substrates (for review, see Henderson and Wolf, 1992). In the present study, the majority of modified genes were downregulated in their expression (21/29), suggesting that pregnancy and lactation may be associated with a decrease in the activity of Phase I DMEs, although the changes in gene expression were dependent on stage.

Gene expression data for Phase II DMEs

The phase II metabolizing or conjugating enzymes include sulfotransferases (SULTs), and UDP-glucuronosyltransferases (UGTs), DT-diaphorase or NAD(P)H:quinone oxidoreductase (NQO) or NAD(P)H:menadione reductase (NMO), epoxide hydrolases (EPHs), glutathione-*S*-transferases (GSTs) and *N*-acetyltransferases (NATs) (Xu et al., 2005). In this study, we also characterized the changes in the expression profiles of Phase II DMEs. During pregnancy and lactation, the expression of 14 phase II DMEs genes was significantly modified. The change in the pattern of expression was the same as that for Phase I DMEs, that is, the major differences in the gene expression of Phase II DMEs occurred either in late pregnancy or at delivery (total of 15 modified, 13 and 10 differentially expressed, respectively), whereas in early pregnancy, moderate differences were observed (only 3 genes differentially expressed), and at peak lactation, no differences. Furthermore, all of the modified genes were downregulated in their expression except for the gene for Sultx3-pending, which showed a marked upregulation in expression on GD 13 and GD 19 (Table 3).

Gene expression data for nuclear receptors

The CYP genes and nuclear receptors form a complex network that may be involved in feedback regulation (Honkakoski and Negishi, 2000). The induction of DMEs occurs primarily at the transcriptional level and is regulated by nuclear receptors that act as ligand-dependent transcription factors (for review, see Handschin and Meyer, 2003). Table 3 shows the differentially regulated NR genes induced during pregnancy and lactation. In late pregnancy,

Table 3
Modified genes for Phase II DMEs and nuclear receptors

Gene family	Accession number	GeneBank definition and comment	Fold change			
			GD 13	GD 19	PPD 0	PPD 14
Nuclear receptor	NM_022186.1	Nuclear receptor-binding factor 2 (Nrbf2)		−1.41		
	NM_057133.1	Nuclear receptor subfamily 0, group B, member 2 (Nr0b2)	−1.8	−2.83		−2.64
	NM_022941.1	Nuclear receptor (CAR) (Nr1i3)	−2.22	−2.14	1.93	
	NM_021745.1	Nuclear receptor subfamily 1, group H, member 4 (Nr1h4)		−1.57		
	NM_052980.1	Nuclear receptor subfamily 1, group I, member 2 (Nr1i2)		−1.62		−1.46
	U20796.1	Nuclear receptor Rev-ErbA-beta mRNA (Nr1d2)		−1.62	1.68	
	AI169222	Nuclear receptor subfamily 1, group H, member 2 (Nr1h2)			−2	
	NM_012576.1	Nuclear receptor subfamily 3, group C, member 1 (Nr3c1)		−1.41		
SULT	NM_031641.1	Sulfotransferase-related protein (Sultx3-pending)	3.03	5.86		
	NM_133547.1	Sulfotransferase family, cytosolic, 1C, member 2 (Sult1c2)		−2	−2	
	AF394783.1	Sulfotransferase SULT1A1		−2		
	AI168953	mRNA for Sulfotransferase K2		−2.83	−2	
GST	M28241.1	Glutathione-*S*-transferase, mu type 2 (Yb2)	−1.74	−2	−2	
	NM_031154.1	Glutathione-*S*-transferase, mu type 3 (Yb3) (Gstm3)	−1.80	−2	−2	
	NM_053293.1	Glutathione-*S*-transferase 1 (theta) (Gstt1)		−2.83	−5.66	
	NM_012796.1	Glutathione-*S*-transferase, theta 2 (Gstt2)	−1.74	−2	−2.07	
	AI169331	Glutathione-*S*-transferase, mu type 2 (Yb2)		−1.96	−3.96	
	BE113459	Highly similar to GTO1_rat glutathione transferase omega 1		−1.52		
	AA945082	Glutathione-*S*-transferase, alpha type (Yc?)			−2	
	NM_017013.1	Glutathione-*S*-transferase, alpha type (Yc?) (Gsta2)			−4	
UDPGT	J02612.1	UDP glycosyltransferase 1 family, polypeptide A6		−1.46		
	AF461738.1	UDP-glucuronosyltransferase 1A7		−2		
EPH	NM_012844	Epoxide hydrolase 1 (microsomal xenobiotic hydrolase) (Ephx1)	−1.57	−1.74	−2.14	

six of eight modified NR genes were downregulated. Two genes were downregulated on GD 13 (Nr0b2 and Nr1i3) and PPD 14 (Nr0b2 and Nr1i2), respectively. Two genes (Nr1i3 and Nr1d2) were upregulated and one gene (Nr1h2) downregulated on PPD 0. The results indicate that most of the altered NR genes were downregulated in their expression in the rat liver in late pregnancy. Therefore, the activities of DMEs, which are mediated by NRs, are likely to be weaker in late pregnancy than at other stages of pregnancy and lactation and in normal virgins. If this timing is confirmed in humans, then these mechanisms are likely less involved in teratogenesis than late fetal growth effects.

Genes involved in oxidative stress

In our previous studies (He et al., 2005a,b), the involvement of increased oxidative stress in the reduction in levels of CYPs during pregnancy and lactation was discussed. Also, a few studies have demonstrated that oxidative stress results in a reduction in the total amount of CYP450 and in drug-metabolizing activities in vivo (Barker et al., 1994; Gatti et al., 1993; Liu et al., 1993). Herein, a microarray analysis was also used to investigate the expression profile of genes implicated in oxidative stress at four different stages. The pathway visualization and analysis tool GenMAPP/MAPPFinder (http://www.GenMAPP.org) was used to identify genes implicated in oxidative stress. Table 4 shows the changes in genes involved in oxidative stress during pregnancy and lactation. All the modified genes belonged to the pathway for the induction of antioxidants and repression of the ROS-producing system. Of eight modified genes, 3 and 5 were significantly decreased except for gene Gclc on GD 19 and PPD 0, respectively, indicating increased oxidative stress. In rats, lipid peroxidation remains low until midpregnancy and begins to rise after day 15 of pregnancy (Sugino et al., 1993). Our results are supported by the investigation of Upreti et al., which indicates that significantly higher lipid peroxidation levels were established in all the major organs of rats during lactation, and early lactation generated higher levels of oxidative stress than late lactation (Upreti et al., 2002).

Table 4
Modified genes implicated in oxidative stress pathway

Gene function	Accession number	GeneBank definition and comment	Fold change			
			GD 13	GD 19	PPD 0	PPD 14
Induction of antioxidant genes	J02612	UDP glycosyltransferase 1 family, polypeptide A6 (Ugt1a6)		−1.46		
	NM_022584.1	Thioredoxin reductase 2 (Txnrd2)			−2	
	J05181.1	Glutamylcysteine gamma synthetase light chain (Gclc)		1.52	1.41	
	NM_012796.1	Glutathione-*S*-transferase, theta 2 (Gstt2)	−1.74	−2	−2.07	
	NM_053906.1	Glutathione reductase (Gsr)			−1.62	
	AA892254	Superoxide dismutase 2, mitochondrial (Sod2)			−1.41	
	NM_012880.1	Superoxide dismutase 3 (Sod3)			−1.32	
Repression of ROS-producing systems	BF420722	Nuclear factor I/X (Nfix)		−2.46		

Verification of results of microarray analysis by quantitative real-time PCR

Real-time PCR was performed as described above using the gene-specific primers listed in Table 1. We chose 9 known genes: 4 from the family of Phase I DMEs (CYP2A1, CYP27, CYP2J3 and CYP4F4), 3 from the family of Phase II DMEs (Ephx1, Gstt1 and Gstm3) and 2 from NRs (Nr1i3 and Nrob2). The results shown in Fig. 2 indicate that the extent of the change detected differed between the microarray and real-time PCR methods. A notable exception was CYP2J3, which exhibited different changes in expression on PPD as assayed with the microarray (no change) or real-time PCR (decrease). Two of the genes validated, Ephx1 and Gstt1, were differentially expressed on GD 19 and PPD 0, respectively. Overall, the real-time PCR analysis validated the results of the microarray analysis, as all the genes examined by both methods were modified during pregnancy and lactation, and eight of nine genes showed similar patterns of change with the two methods.

Comment

Taken together, the expression of a large number of genes encoding DMEs and NRs was decreased in rat liver especially in late pregnancy and early lactation, suggesting decreased activities of DMEs. This is supported by previous studies (Dean and Stock, 1975; Dean et al., 1989; Feuer and Liscio, 1969; Guarino et al., 1969; Neale and Parke, 1973). Furthermore, consistent with the present data, protein levels of some CYPs have been shown to be reduced during pregnancy and lactation in rat liver (He et al., 2005a,b). An investigation by Kishi et al. also suggests that pregnancy had a negative effect on cytochrome P450 content at a late stage (Kishi et al., 2005). At present, it is not known how pregnancy and lactation are involved in regulating the expression of genes encoding DMEs. Further elucidation of pregnancy and lactation-induced changes in gene expression will help to better understand these physiological processes and possibly provide the basis for drug safety during pregnancy and lactation.

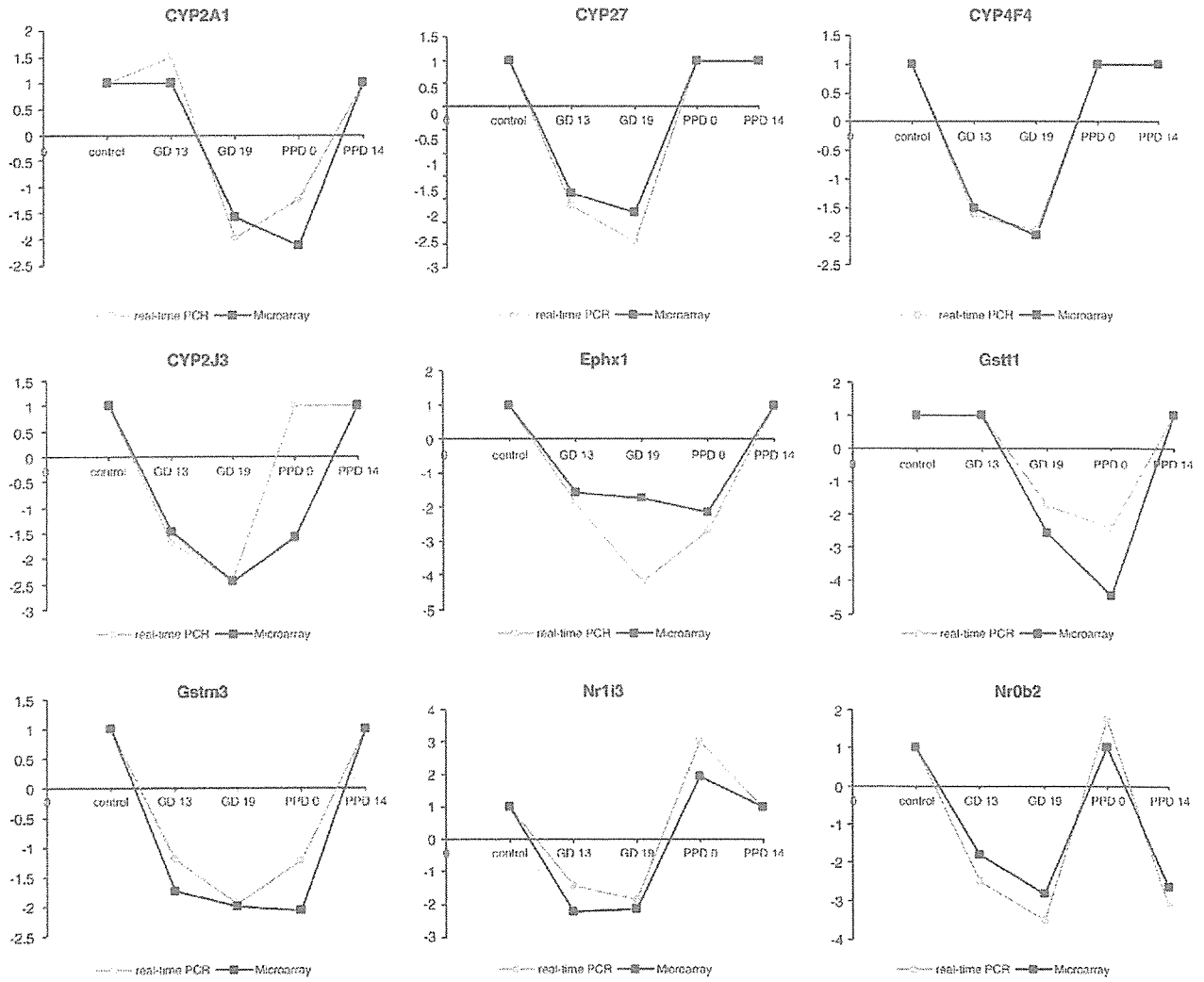

Fig. 2. Comparison of RNA levels for selected genes from Phases I and II DMEs and NRs by microarray analysis and real-time PCR. Data are presented as fold change from levels in virgin control rats. Real-time PCR data are shown as the mean of triplicate measurements.

Future studies in the clinical setting in patients will be necessary to determine how fully these results and insights, derived in a short gestational mammalian model, apply to the biological imperatives of human pregnancy in the nutritional, environmental, and pharmacological circumstances of modern times (Shanklin, 2000).

References

Abel, E.L., et al., 1979. Influence of lactation on rate of disappearance of ethanol in the rat. Neurobehav. Toxicol. 1, 185–186.

Barker, C.W., et al., 1994. Down-regulation of P4501A1 and P4501A2 mRNA expression in isolated hepatocytes by oxidative stress. J. Biol. Chem. 269, 3985–3990.

Christopher, F., Gertie, FM., 1998. Physiological changes associated with pregnancy. Updat. Anaesth. 1–6.

Dean, M.E., Stock, B.H., 1975. Hepatic microsomal metabolism of drugs during pregnancy in the rat. Drug Metab. Dispos. 3, 325–331.

Dean, M., et al., 1989. The pharmacokinetics of salicylate in the pregnant Wistar rat. Drug Metab Dispos. 17, 87–90.

Ejiri, N., et al., 2005a. Microarray analysis on CYPs expression in pregnant rats after treatment with pregnenolone-16alpha-carbonitrile and phenobarbital. Exp. Mol. Pathol. 78. 71–77.

Ejiri, N., et al., 2005b. Microarray analysis on Phase II drug metabolizing enzymes expression in pregnant rats after treatment with pregnenolone-16alpha-carbonitrile or phenobarbital. Exp. Mol. Pathol. 79, 272–277.

Elenkov, I.J., et al., 2001. IL-12, TNF-alpha, and hormonal changes during late pregnancy and early postpartum: implications for autoimmune disease activity during these times. J. Clin. Endocrinol. Metab. 86, 4933–4938.

Escalada, J., et al., 1996. Prolactin gene expression and secretion during pregnancy and lactation in the rat: role of dopamine and vasoactive intestinal peptide. Endocrinology 137, 631–637.

Feuer, G., Liscio, A., 1969. Origin of delayed development of drug metabolism in the newborn rat. Nature 223, 68–70.

Frederiksen, M.C., 2001. Physiologic changes in pregnancy and their effect on drug disposition. Semin. Perinatol. 25, 120–123.

Gatti, S., et al., 1993. Role of tumour necrosis factor and reactive oxygen intermediates in lipopolysaccharide-induced pulmonary oedema and lethality. Clin. Exp. Immunol. 91, 456–461.

Guarino, A.M., et al., 1969. Alterations in kinetic constants for hepatic microsomal aniline hydroxylase and ethylmorphine *N*-demethylase associated with pregnancy in rats. J. Pharmacol. Exp. Ther. 168, 224–228.

Handschin, C., Meyer, U.A., 2003. Induction of drug metabolism: the role of nuclear receptors. Pharmacol. Rev. 55, 649–673.

He, X.J., et al., 2005a. Changes in cytochrome P450 isozymes (CYPs) protein levels during lactation in rat liver. Exp. Mol Pathol. 79. 224–228.

He, X.J., et al., 2005b. Effects of pregnancy on CYPs protein expression in rat liver. Exp. Mol. Pathol. 78, 64–70.

Henderson, C., Wolf, C.R., 1992. Progress in Drug Metabolism. Taylor and Francis, London.

Honkakoski, P., Negishi, M., 2000. Regulation of cytochrome P450 (CYP) genes by nuclear receptors. Biochem. J. 347, 321–337.

Jahn, G.A., et al., 1991. Prolactin receptor gene expression in rat mammary gland and liver during pregnancy and lactation. Endocrinology 128, 2976–2984.

Kishi, R., et al., 2005. Effects of pregnancy, age and sex in the metabolism of styrene in rat liver in relation to the regulation of cytochrome P450 enzymes. J. Occup. Health 47, 49–55.

Liu, P.T., et al., 1993. The effects of ether anaesthesia on oxidative stress in rats-dose response. Toxicology 80, 37–49.

Loebstein, R.L.A., Koren, G., 1997. Pharmacokinetic changes during pregnancy and their clinical relevance. Clin. Pharmacokinet. 33, 328–343.

Neale, M.G., Parke, D.V., 1973. Effects of pregnancy on the metabolism of drugs in the rat and rabbit. Biochem. Pharmacol. 22, 1451–1461.

Nelson, D.R., et al., 1993. The P450 superfamily: update on new sequences, gene mapping, accession numbers, early trivial names of enzymes, and nomenclature. DNA Cell Biol. 12, 1–51.

Sakaguchi, K., et al., 1998. Tissue-specific regulation of growth hormone receptor and growth hormone binding protein gene expression during pregnancy and lactation in the rat. Endocr. J. 45, S105–S107 (Suppl.).

Shanklin, D.R., 2000. Maternal nutrition and child health. Charles C. Thomas, Springfield, IL. pp. 9–10, 223–242.

Smith, R.W., 1975. The effects of pregnancy and lactation on the activities in rat liver of some enzymes associated with glucose metabolism. Biochim. Biophys. Acta 411, 22–29.

Sugino, N., et al., 1993. Changes in activities of superoxide dismutase and lipid peroxide in corpus luteum during pregnancy in rats. J. Reprod. Fertil. 97, 347–351.

Travers, M.T., et al., 1993. Regulation of serum insulin-like growth factor-I (IGF-I), hepatic growth hormone binding and IGF-I gene expression in the rat during pregnancy and lactation. J. Endocrinol. 139, 89–95.

Upreti, K., et al., 2002. Evaluation of peroxidative stress and enzymatic antioxidant activity in liver and kidney during pregnancy and lactation in rats. Health Popul., Perspect. Issues 25, 177–185.

Xiao, X.Q., et al., 2004. Metabolic adaptations in skeletal muscle during lactation: complementary deoxyribonucleic acid microarray and real-time polymerase chain reaction analysis of gene expression. Endocrinology 145, 5344–5354.

Xu, C., et al., 2005. Induction of phase I, II and III drug metabolism/transport by xenobiotics. Arch. Pharm. Res. 28, 249–268.

European Journal of Neuroscience, Vol. 24, pp. 2758–2768, 2006 doi:10.1111/j.1460-9568.2006.05161.x

Repair process of fetal brain after 5-azacytidine-induced damage

Masaki Ueno, Kei-ichi Katayama, Hirofumi Yamauchi, Akira Yasoshima, Hiroyuki Nakayama and Kunio Doi
Department of Veterinary Pathology, Graduate School of Agricultural and Life Sciences, The University of Tokyo, 1-1-1 Yayoi, Bunkyo-ku, Tokyo 113-8657, Japan

Keywords: apoptosis, damage, developing brain, microglia, rat, repair

Abstract

The fetal brain is susceptible to many extrinsic stresses. Some of these stresses induce excessive cell death in the prenatal stage, leading to anomalies in the neonatal brain. However, it is unclear how the developing brain responds to and repairs the prenatal tissue damage. We treated pregnant rats on day 13 of gestation with 5-azacytidine, one of the compounds that induces excessive cell death and inhibits proliferation in neural progenitor cells, to damage the fetal brain, and investigated the repair process up to 60 h after treatment. Histological analysis showed that 5-azacytidine induced strong apoptosis of neural cells. By 60 h, apoptotic cells disappeared and the tissue was repaired, although the telencephalic wall remained thinner than in controls. Flow cytometry analysis showed that the cell cycle distribution also returned to control levels at 60 h, suggesting that the repair process was completed around 60 h. During the repair period, amoeboid microglia infiltrated the brain and ingested the apoptotic cells. These microglial cells were positive for the multiple microglial markers, and mRNAs for the microglia-related cytokines tumor necrosis factor α, interleukin 1β and macrophage colony stimulating factor (M-CSF) were up-regulated. DNA microarray analysis showed the up-regulation of genes relevant to glial cells, inflammation, the extracellular matrix, glycolysis, proliferation and neural development. We show here that the developing brain has the capacity to respond to the damage induced by extrinsic chemical stresses, including changing the expression of numerous genes and the induction of microglia to aid the repair process.

Introduction

The fetal central nervous system (CNS) is sensitive to a number of environmental factors that can influence normal CNS development (Rodier, 1995; Mendola *et al.*, 2002; Costa *et al.*, 2004). Extrinsic cytotoxic stresses (e.g. irradiation, ethanol, heavy metals and genotoxic agents) can disrupt many events which occur during development, i.e. proliferation, migration and differentiation. One of the most severe effects of these stresses is the suppression of cell proliferation and the induction of excessive cell death in the prenatal developing brain. This damage leads to structural abnormalities such as reduction in brain size, disorganization of cortical lamina and dilatation of the ventricles after birth (Choi, 1989; Sun *et al.*, 1996; Kimler, 1998; Katayama *et al.*, 2000, 2005a, b; Guerri, 2002; Ueno *et al.*, 2006).

Although the mechanisms of fetal brain injury and features of brain abnormalities after birth have been well studied, the processes between these stages remain unclear. We hypothesize that the fetal CNS has the ability to repair itself postinjury because, even if the fetal brain suffers damage, most of the structures of the brain remain after birth, although some abnormalities are observed. In the adult brain, it is well known that the CNS harbors the ability to repair itself. Activation of microglia and subsequent astrocytes are involved in the repair process (Fawcett & Asher, 1999; Silver & Miller, 2004). Further, there has been a recent focus on regeneration of neural cells in the adult brain (Magavi *et al.*, 2000; Doetsch, 2003; Picard-Riera *et al.*, 2004). However, although a few researchers have studied the repair period in the developing brain (Oyanagi *et al.*, 1998; Kikuchi-Horie *et al.*, 2004), it is not widely known how the developing brain responds to extrinsic damage or how the repair or recovery process is regulated.

To study the repair process after fetal brain damage, we exposed fetal rat brains to 5-azacytidine (5AzC), one of the compounds that induces excessive cell death and inhibits cell cycle progression in neural progenitor cells (Ueno *et al.*, 2006), and examined the resulting recovery and changes in histology and cell proliferation. We then investigated the role of microglia and cytokines in the repair process, as microglial precursors appear in the neuroepithelium at around embryonic day 11 (Ashwell, 1991; Sorokin *et al.*, 1992; Alliot *et al.*, 1999; Kaur *et al.*, 2001), and are activated in the injured fetal brain (Hao *et al.*, 2001a). Finally, we performed DNA microarray analysis to identify the genes that are activated during the repair process in the developing brain. Our results indicate that the developing brain can respond to and repair the damaged tissue by changing the expression of numerous genes and activation of microglial cells.

Materials and methods

All procedures were approved by the Animal Care and Use Committee of the Graduate School of Agricultural and Life Sciences, The University of Tokyo.

Animals

Pregnant Jcl:Wistar rats were obtained from Japan CLEA (Tokyo, Japan).

Correspondence: Dr Masaki Ueno, as above.
E-mail: ms-ueno@umin.ac.jp

Received 6 April 2006, revised 31 August 2006, accepted 4 September 2006

Chemical

The 5AzC was obtained from Sigma (St Louis, MO, USA).

Treatment

On day 13 of gestation, pregnant rats were injected intraperitoneally with 10 mg/kg of 5AzC and then killed by exsanguination under ether anesthesia at 24, 36, 48 or 60 h after treatment. This dose was selected because it induces widespread neural apoptosis with low fetal mortality (Lu *et al.*, 1998). Control dams were injected with an equivalent volume of saline and killed at the same times after treatment.

Histopathology and immunohistochemistry

Collected fetuses were fixed in 10% neutral-buffered formalin and embedded in paraffin. Paraffin sections (thickness 4 μm) were stained with hematoxylin and eosin for histopathological examination or immunostained for ED-1 and Iba-1, markers of microglia, glial fibrillary acidic protein (GFAP), a marker of astrocytes, and osteopontin by the labeled streptavidin biotin (LSAB) method with streptavidin (Dako, Carpinteria, CA, USA). For preparation of frozen sections, fetuses were fixed in 2% periodate-lysine-paraformaldehyde for 6 h and then incubated in 15% sucrose/phosphate-buffered saline overnight. They were then embedded in O.C.T. compound (Sakura, Tokyo, Japan) and kept at −80 °C until used. Frozen sections (6 μm thick) were used for immunohistochemical staining for ED-1 and CD11b, markers of microglia, by the LSAB method. Mouse anti-ED-1 monoclonal antibody (BMA Biomedicals, Augst, Switzerland), rabbit anti-Iba-1 polyclonal antibody (Wako, Osaka, Japan), mouse anti-CD11b monoclonal antibody (Serotec, Oxford, UK), rabbit anti-GFAP polyclonal antibody (Dako) and rabbit anti-osteopontin (IBL, Fujioka, Japan) were used as the primary antibodies, and biotin-labeled goat anti-rabbit/mouse IgG (Kirkegaard & Perry, Gaithersburg, MD, USA) was used as the secondary antibody. Signals were visualized by using a peroxidase diaminobenzidine reaction and the sections were counterstained with methyl green. For double staining, fluorescein isothiocyanate-labeled anti-rabbit IgG (Santa Cruz, Santa Cruz, CA, USA) and biotin-labeled goat anti-mouse IgG (Kirkegaard & Perry) with rhodamine-labeled avidin (Vector, Burlingame, CA, USA) were used as the secondary antibodies. The index of microglial cells (the number of ED-1- or Iba-1-positive cells/mm^2) was represented as the mean + SD of three embryos from different dams and statistical analysis was performed by Student's *t*-test.

TUNEL method

Cells with DNA fragmentation (apoptotic cells) were detected by the TUNEL method, using an apoptosis detection kit (Apop Tag; Chemicon, Temecula, CA, USA). In brief, multiple fragmented DNA 3′-OH ends on each fetal paraffin section (thickness 4 μm) were labeled with digoxigenin-dUTP in the presence of terminal deoxynucleotidyl transferase. Peroxidase-conjugated anti-digoxigenin antibody was then reacted with the sections. Apoptotic nuclei were visualized by a peroxidase–diaminobenzidine reaction and sections were then counterstained with methyl green. The apoptosis index (%) (number of TUNEL-positive cells/500 cells) was represented as the mean ± SD of three embryos from different dams and statistical analysis was performed by Student's *t*-test.

Lectin staining and electron microscopy

Fetuses were fixed in 4% paraformaldehyde for light microscopic examination or 1% paraformaldehyde/1% glutaraldehyde for electron microscopy for 6 h and then incubated in 15% sucrose/phosphate-buffered saline overnight. They were then embedded in O.C.T. compound (Sakura) and kept at −80 °C until used. Peroxidase-conjugated BS-I (lectin from *Bandeiraea simplicifolia*; 10 μg/mL; Sigma) was used for detecting microglial cells. Cryosections (thickness 8 μm) were washed in Tris-buffered saline and placed in 0.3% H_2O_2/methanol for 30 min to inactivate endogenous peroxidases. Sections were then incubated in 8% skim milk/Tris-buffered saline for 40 min to reduce non-specific staining and incubated in BS-I overnight at 4 °C. The sections were visualized by a peroxidase–diaminobenzidine reaction and then counterstained with methyl green. For electron microscopic examination, lectin-stained sections were postfixed in 1% osmium tetroxide in 0.2 M phosphate buffer (PB) for 2.5 h. After dehydration through an ascending ethanol series and propylene oxide, tissues were embedded in Epok 812 resin (Oken Co., Tokyo, Japan). Ultrathin sections were double-stained with uranyl acetate and lead citrate, and observed under a JEOL-1200EX electron microscope (JEOL, Tokyo, Japan).

Cell cycle analysis

The telencephalons from two fetuses of each dam (24–60 h after treatment) were obtained carefully under stereoscopic microscopy and divided into two parts, one containing the dorsal to lateral telencephalic wall and one containing the basal ganglia. They were then prepared for flow cytometric analysis as described previously (Ueno *et al.*, 2006). In brief, the cells were fixed in 70% ethanol at 4 °C overnight. Cells were then incubated with ribonuclease A (250 μg/mL, Sigma) for 40 min at 37 °C and stained with propidium iodide (50 μg/mL, Sigma) for 30 min on ice. Cell cycle analysis was performed by using the FACS Calibur system (Becton Dickinson, Mountain View, CA, USA) and cell cycle distribution was analysed by using the CELL QUEST program (Becton Dickinson). The percentage for each cell cycle phase was represented as the mean ± SD of three dams and statistical analysis was performed by Student's *t*-test.

RNA extraction and microarray analysis

Microarray expression analysis was performed with the GeneChip system (Affymetrix, Santa Clara, CA, USA) according to the manufacturer's instructions. Six to eight fetal telencephalons were acquired from each dam (24, 36 or 48 h after treatment, and controls; $n = 2$ dams per time point) and total RNA was extracted with the RNeasy Mini Kit (Qiagen, Germantown, MD, USA). The quality and quantity of the extracted RNA samples were examined by agarose gel electrophoresis. Double-stranded cDNA was then synthesized from the total RNA. The first cDNA strand was prepared from 10 μg of total RNA with SuperScript II RNase H$^-$ reverse transcriptase (Invitrogen, Carlsbad, CA, USA) and the T7-$(dT)_{24}$ primer (primer sequence, 5′-GGCCAGTGAATTGTAATACGACTCACTATAGGGAGGCGG-$[dT]_{24}$-3′, Amersham Bioscience, Tokyo, Japan). The second strand was synthesized with the SuperScript double-stranded cDNA synthesis kit (Invitrogen). Biotin-labeled cRNA was then synthesized from the double-stranded cDNA with the high-yield RNA transcription labeling Kit (Enzo Diagnostics, NY, USA) and purified with the RNeasy Mini Kit (Qiagen). Biotin-labeled cRNA (20 μg) was then fragmented in fragmentation buffer and mixed in a hybridization

solution prepared with a GeneChip eukaryotic hybridization control kit (Affymetrix). cRNA was hybridized to the Affymetrix rat expression array 230A for 16 h at 45 °C while being rotated at 60 r.p.m. in a GeneChip hybridization oven 640 (Affymetrix). The chips were then washed and stained automatically with a Fluidics station (Affymetrix) and scanned with the GeneArray scanner (Hewlett Packard, Palo Alto, CA, USA).

Microarray data analysis

Microarray imaging data were analysed with MICROARRAYSUITE v. 5.0 (Affymetrix). After hybridization intensity data were captured, the intensity values of each probe were calculated automatically. Data were scaled, normalized and then compared between the treated and control groups. In the pairwise comparison of results from the two microarrays, the patterns of change of the whole probe set were used to perform statistical analysis as described in the manufacturer's guide (MICROARRAYSUITE v. 5.0 User's Guide) and a qualitative call (a 'difference call') of increase, decrease, marginal increase, marginal decrease or no change was made. We then extracted the groups of genes corresponding to increase, marginal increase, decrease or marginal decrease in both samples at each time point and performed clustering (http://rana.lbl.gov/EisenSoftware.htm) and pathway (http://www.GenMAPP.org) analyses. The change in gene expression was calculated as the ratio of the average value from experimental arrays compared with control arrays.

Real-time polymerase chain reaction and polymerase chain reaction

Total RNA was reverse-transcribed for first-strand cDNA synthesis with an oligo $(dT)_{12-18}$ primer and SuperScript II RNase H$^-$ reverse transcriptase (Invitrogen). Real-time polymerase chain reaction (PCR) was performed with oligonucleotide primer sets corresponding to the cDNA sequences of: *Mif* (NM_031051.1), *Lgals3* (NM_031832.1), *osteopontin* (AB001382.1), *P4ha1* (BI274401), *Pkm2* (NM_053297.1), *Fgf15* (NM_130753.1) and glyceraldehyde-3-phosphate dehydrogenase (*GAPDH*). Sense and antisense primers were as follows:

Mif-1, 5′-CAAGCCGGCACAGTACATCG-3′ and
5′-GGTCGCTCGTGCCACTAAAAG-3′;
Lgals3, 5′-GACCACTTCAAGGTTGCGGTC-3′ and
5′-GGAAGCGCTGGTGAGGGTTAT-3′;
osteopontin, 5′-CTGTCTCCCGGTGAAAGTGG-3′ and
5′-GAGATGGGTCAGGCTTCAGC-3′;
P4ha1, 5′-CAGGCTGAGCCGAGCTACA-3′ and
5′-CATAGCCAGACAGCCAAGCAC-3′;
Pkm2, 5′-GGAGGCCAGCGATGGAATC-3′ and
5′- CTGGGTGGCGCAGATGACT-3′;
Fgf15, 5′-GGGCTGATTCGCTACTCGG-3′ and
5′-GGTGGTGCTTCATGGACCTGT-3′;
and *GAPDH*, 5′- CCTGCACCACCAACTGCTTAG-3′ and
5′- CATGGACTGTGGTCATGAGCC-3′.

In brief, 25 μL of reaction mixture containing 12.5 μL SYBR green real-time PCR master mix (Toyobo, Osaka, Japan), 0.2 μM each of the sense and antisense primers, and 1 μL of the cDNA sample was preheated at 95 °C for 3 min and then underwent 40 cycles of amplification (denaturation at 95 °C for 15 s, annealing and extension at 60 °C for 1 min) with an ABI PRISM 7900HT sequence detection system (Applied Biosystems, Foster City, CA, USA). The relative intensity against *GAPDH* was calculated and the fold change relative to control was shown as the mean + SD from three dams. Statistical analysis was performed by Student's *t*-test.

Polymerase chain reaction was performed using oligonucleotide primer sets corresponding to the cDNA sequences of tumor necrosis factor-α (*TNF-α*) (NM_012675.1), interleukin-1β (*IL-1β*) (NM_031512.1), macrophage colony stimulating factor (*M-CSF*) (AF514356) and *GAPDH*. Sense and antisense primers were as follows:

TNF-α, 5′-GCTCTTCTGTCTACTGAACTTCG-3′ and
5′-CAGCCTTGTCCCTTGAAGAGAA-3′ (36 cycles);
IL-1β, 5′-GATTGCTTCCAAGCCCTTGACT-3′ and
5′-AGGTGGAGAGCTTTCAGCTCA-3′ (36 cycles);
M-CSF, 5′-CTCTCCCCATTTTGCCAC-3′ and
5′-TCCTCCGCTTCCAACTGTA-3′ (34 cycles); and
GAPDH, 5′-GAGTATGTCGTGGAGTCTACTG-3′ and
5′- GCTTCACCACCTTCTTGATGTC-3′ (21 cycles).

In brief, 100 μL of reaction mixture containing 10 μL 10 × PCR buffer (100 mM Tris.HCl buffer, 500 mM KCl and 15 mM $MgCl_2$; Takara, Shiga, Japan), 10 μL dNTP (Takara), 50 pmol each of sense and antisense primers, and 1 μL of the cDNA sample were preheated at 95 °C for 5 min, and a PCR reaction cycle (× each cycle number) of denaturation at 95 °C for 1 min, annealing at 58 °C for 1 min and extension at 72 °C for 1 min was performed in a PCR thermal cycler SP (Takara). The PCR products were electrophoresed and stained with ethidium bromide.

Results

Histopathological changes

We performed all analyses on the telencephalon because histopathological changes after 5AzC treatment there reflect changes in other areas of the CNS, including the diencephalon, mesencephalon and metencephalon (Ueno *et al.*, 2002b). 5AzC induces apoptosis in the proliferating neural progenitor cells in the ventricular zone (VZ) from 6 to 12 h after treatment (Ueno *et al.*, 2002a, 2006). Apoptosis is then induced in differentiating neural cells in the cortical plate, outside the VZ, at 24 h after treatment (Ueno *et al.*, 2002a). The number of apoptotic cells peak between 12 and 24 h after treatment (Ueno *et al.*, 2002a).

To elucidate the repair process after the injury, we examined the histological changes after 5AzC-induced cell death in two main areas of the telencephalon, the telencephalic wall and the basal ganglia (see Fig. 3A, a) at various time points between 24 and 60 h. The number of apoptotic cells, defined as cells positive for TUNEL staining, gradually decreased from a peak at 24 h (Fig. 1, Ab and Aj and C). Most apoptotic cells were observed in the differentiating field (DF), where postmitotic neural cells are located (arrowheads in Fig. 1, Ab, Ad, Af and Bb; in the telencephalic wall, this field is generally called the cortical plate or marginal zone), although there were also some in the VZ. From 24 to 48 h, many aggregating bodies of apoptotic cells were observed in the VZ and DF (arrowheads in Fig. 1, Bb and Bc). At 48 h, the apoptotic cells in the telencephalic wall had almost completely disappeared (Fig. 1, Af) but were still present in the basal ganglia. By 60 h, no apoptotic cells were detected in the telencephalon but the thickness of the telencephalic wall was remarkably decreased (Fig. 1, Ag and Ah). These results indicate that the recovery from 5AzC-induced damage is complete by around 60 h and that the process of brain development continues.

Cell cycle analysis

We then performed cell cycle analysis using flow cytometry to evaluate the activity of proliferation after the insult. In the telencephalic wall, many apoptotic cells in the sub-G1 phase were observed at 24 h (control, 0.9 ± 0.1%; 5AzC, 12.6 ± 0.6%) and thereafter the number of apoptotic

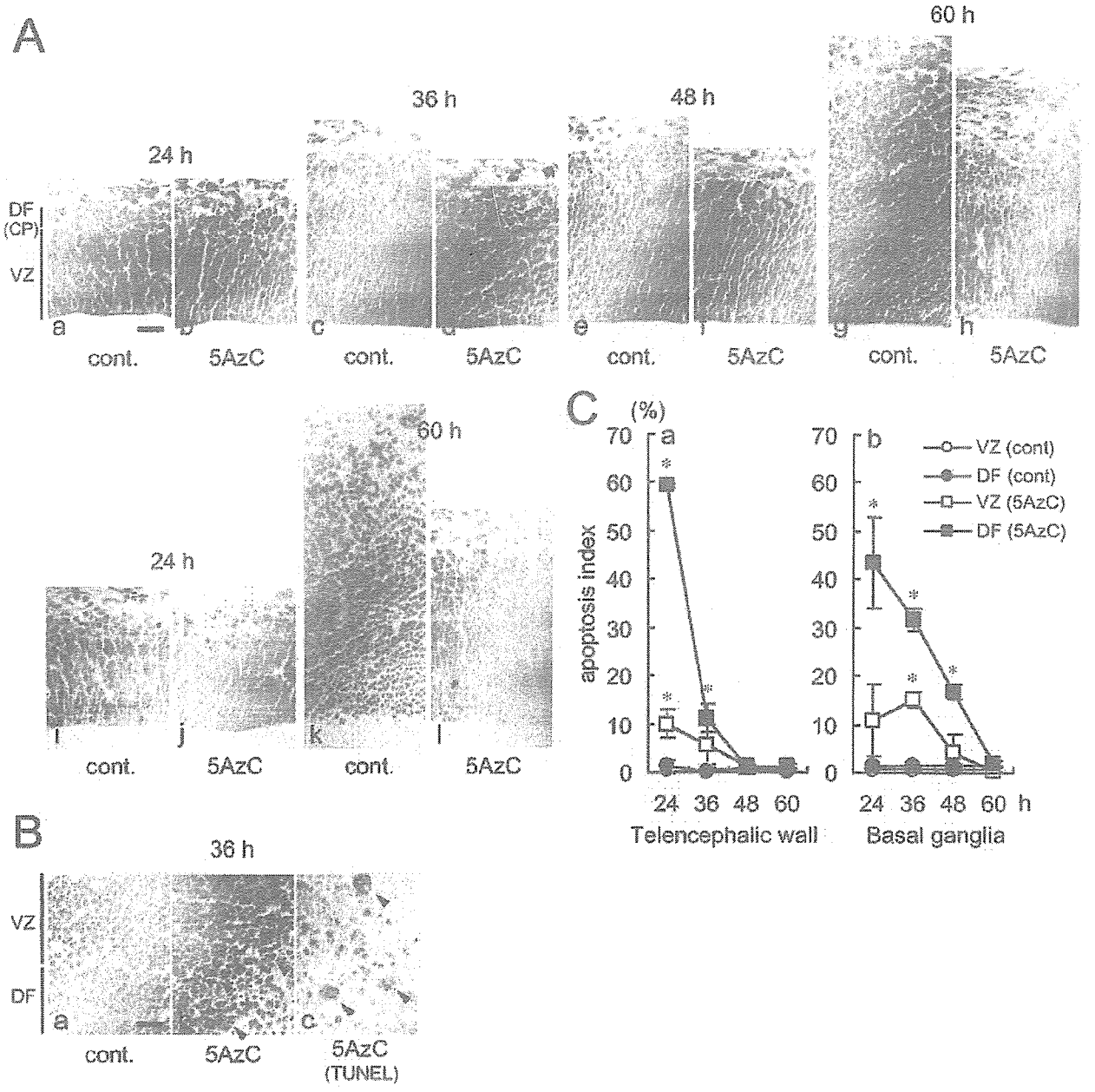

FIG. 1. Histopathological changes in the telencephalon of 5-azacytidine (5AzC)-treated rat fetuses. (A) The telencephalic wall (a, b, i and j, 24 h; c and d, 36 h; e and f, 48 h; g, h, k and l, 60 h) was stained by hematoxylin and eosin (a–h) or TUNEL (i–l). At each time point, the left panel is the control and the right panel is 5AzC-treated tissue. Apoptotic cells were observed mainly in the differentiating field (DF) [or cortical plate (CP)] (arrowheads in b, d and f). The thickness of the telencephalic wall was remarkably decreased at 60 h (g and h). VZ, ventricular zone. Scale bar, 50 μm. (B) The basal ganglia (36 h) were stained by hematoxylin and eosin (a and b) or TUNEL (c). (a) Control; (b and c) 5AzC-treated group. Aggregating bodies of apoptotic cells were observed (arrowheads in b and c). Scale bar, 50 μm. (C) Apoptosis index. TUNEL-positive apoptotic cells were counted in the VZ (open symbol) and DF (closed symbol) of control (circle) and 5AzC-treated (square) telencephalic wall (a) and basal ganglia (b). The apoptosis index (%) (number of TUNEL-positive cells/500 cells) represents the mean + SD of three embryos from different dams. $^*P < 0.05$: significantly different from control (Student's *t*-test).

cells decreased remarkably (Fig. 2a and c). The number of S-phase cells increased between 24 and 48 h (Fig. 2a and c; control: 24 h, 18.6 ± 0.4%; 36 h, 19.0 ± 1.4%; 48 h, 16.5 ± 0.8%; 5AzC: 24 h, 29.5 ± 5.2%; 36 h, 24.6 ± 4.3%; 48 h, 22.1 ± 0.7%). At 60 h, the distribution of cells in each cell cycle stage recovered close to control levels (Fig. 2a and c; control: sub-G1, 0.9 + 0.1%; G0/G1, 74.3 + 4.7%; S, 16.9 ± 3.6%; G2/M, 7.9 ± 1.1%; 5AzC: sub-G1, 1.1 ± 0.4%; G0/G1, 72.1 ± 0.8%; S, 17.0 ± 1.4%; G2/M, 9.7 ± 0.2%).

In the basal ganglia, the number of apoptotic cells reached a peak at 36 h (Fig. 2b and d; control, 0.6 + 0.3%; 5AzC, 7.6 ± 0.6%) and then decreased. This peak occurred later than in the telencephalic wall

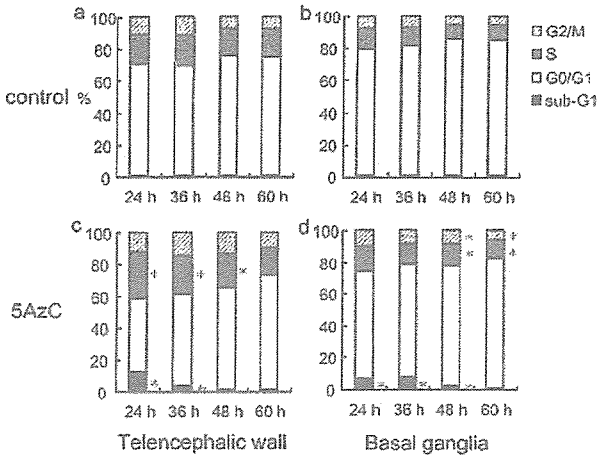

FIG. 2. Cell cycle analysis of telencephalic cells in the rat fetus [a and c, telencephalic wall; b and d, basal ganglia; a and b, control; c and d, 5-azacytidine (5AzC)-treated]. Percentages for each cell cycle phase are presented as the mean of three dams (hatched bar: G2/M; grey bar: S; white bar: G0/G1; black bar: sub-G1). 5AzC treatment increased the number of S-phase cells and apoptotic cells in the sub-G1 area, and cell cycle distribution returned close to control levels at 60 h. $^{*}P < 0.05$; significantly different from control (Student's *t*-test).

(12–24 h) and paralleled changes in histopathology (Fig. 1C). The proportion of S- and G2/M-phase cells increased at 48 h (Fig. 2b and d; control: S, 8.8 ± 0.3%; G2/M, 5.1 ± 0.9%; 5AzC: 48 h, 13.7 ± 3.0%, G2/M, 8.3 ± 0.3%) and remained slightly elevated at 60 h, although the overall cell cycle distribution was similar to that in controls (Fig. 2b and d; control: sub-G1, 0.4 ± 0.1%; G0/G1, 85.2 ± 1.1%; S, 9.0 ± 0.9%; G2/M, 5.4 ± 0.3%; 5AzC: sub-G1, 1.1 ± 0.3%; G0/G1, 81.6 ± 0.2%; S, 11.1 ± 0.1%; G2/M, 6.3 ± 0.1%). These results indicate that the restoration of normal cell cycle control following 5AzC treatment is completed by 60 h, which is consistent with the histopathological results.

Detection of microglia

The above-mentioned histological and cell cycle analyses suggested that tissue damage could be repaired and recovered in the fetal brain. Next, to clarify which types of cell contribute to the recovery or repair phase, we focused on the role of microglia. Microglia have two states, active amoeboid and resting ramified type (Ling & Wong, 1993). It is known that, after embryonic day 11, amoeboid microglia infiltrate the developing brain from the surrounding tissues and some of them ingest the apoptotic cells that form during normal brain development (Ashwell, 1991). These cells are activated by chemical-induced damage (Hao *et al.*, 2001a). To investigate the distribution of microglia in the 5AzC-injured fetal brain, we labeled cells for the multiple microglial markers ED-1, CD11b, Iba-1 and lectin (BS-I) (Fig. 3A; Hao *et al.*, 2001a; Imai & Kohsaka, 2002).

In the control telencephalon, cells positive for Iba-1 or BS-I were observed in the VZ, DF, ventricle and surrounding mesenchymal tissue (Fig. 3, Aa). Cells in the ventricle were round (amoeboid type), whereas cells in other areas were dendritic or spindled (ramified type, Fig. 3, Aa, Ca and Da). ED-1-positive cells were observed mainly in the mesenchymal tissues around the brain, with only a few positive cells in the telencephalon.

Treatment with 5AzC increased the number of microglia in the telencephalon (Fig. 3, Ab–Af). The number of ED-1-positive cells in the telencephalic wall increased from 24 h after 5AzC treatment and increased after 36 h in the basal ganglia (Fig. 3, Ba and Bb). In contrast, the number of Iba-1-positive cells did not increase remarkably in the basal ganglia but did increase in the telencephalic wall (Fig. 3, Aa, Ab, Be and Bd), suggesting that 5AzC treatment activates microglia in the basal ganglia but does not dramatically increase cell proliferation. Indeed, double-staining with ED-1 and Iba-1 showed Iba-1 single-positive cells with ramified morphology in the control basal ganglia (Fig. 3, Ca) but double-positive cells with amoeboid morphology in the 5AzC group (Fig. 3, Cb), indicating that injury activates Iba-1-positive microglia, followed by expression of ED-1 and subsequent morphological changes.

The aggregated bodies composed of apoptotic cells were also positive for these markers [Figs 1, Bb and Be (arrowheads) and 3, Ae, Af and Cb], suggesting that these aggregates are microglia that have ingested apoptotic cells. To confirm this hypothesis, we performed electron microscopy with BS-I staining. Between 24 and 48 h, phagocytotic cells positive for lectin in the cytoplasmic membrane were observed (Fig. 3, Db). Some cells had ingested many apoptotic bodies, indicating that these aggregating bodies were lectin-positive microglia. Their shapes were rounded like amoeboid microglia, whereas dendritic or spindle-type microglia were observed in control brains (Fig. 3, Ca and Da).

In the telencephalic wall, most microglia were observed in the DF (corresponding to the cortical plate) along the pia mater (Fig. 3, Ab–Ad), indicating that microglia infiltrated from surrounding mesenchymal tissues. In the basal ganglia, most microglia assembled at the boundary of the VZ and DF, where apoptosis primarily occurred (Fig. 3, Ab, Ae and Af), whereas they were diffusely distributed in the controls (Fig. 3, Aa). These results indicate that microglia normally residing in the basal ganglia migrated into the injured area and were transformed into phagocytotic cells.

Expression of cytokines

To investigate the key molecules that engage in activating microglia in the damaged embryonic brain, we determined the expression levels of three cytokines (TNF-α, IL-1β and M-CSF) that play roles in microglial induction, proliferation and activation (Burns *et al.*, 1993; Hao *et al.*, 2001a,b, 2002; Nakajima & Kohsaka, 2001; Hanisch, 2002). The mRNA levels of all cytokines were up-regulated. *TNF-α* increased between 24 and 60 h, *IL-1β* between 24 and 36 h, and *M-CSF* between 24 and 48 h (Fig. 4), suggesting that microglia were activated by these cytokines.

Detection of astrocytes

The astrocyte is the other type of glial cell that mediates the repair of lesions in the adult brain. To confirm the presence of astrocytes in the repair process of fetal brain, we labeled cells for GFAP, a marker of astrocytes. However, we could not detect any GFAP-positive astrocytes after 5AzC-induced damage (Fig. 5). The mRNA expression of astrocyte markers *GFAP* and *S100β* was analysed in greater detail with DNA microarray analysis but their expression levels were not elevated throughout the experimental period (data not shown). These results suggest that astrocytes do not participate in the repair process in the fetal brain at least from embryonic day 13 to 15.

Gene expression in the repair process

We further used DNA microarray analysis to determine which genes were modulated in the repair process. According to the criteria